PHOTOGRAPH THIS SHEET

AD A950860

DTIC ACCESSION NUMBER

LEVEL

INVENTORY

Massachusetts Inst. of Tech., Cambridge

Feasibility of Compact 4MEV Electrostatic X-Ray Source Studies of Compressed Gas and High Vacuum - - -

DOCUMENT IDENTIFICATION

Supplementary Final Rpt., Jun. 52 - Jun. 54 1 Dec 54

Contract DA19-020-ORD2023 WAL-142/58-8

DISTRIBUTION STATEMENT A
Approved for public release;
Distribution Unlimited

DISTRIBUTION STATEMENT

ACCESSION FOR	
NTIS GRA&I	X
DTIC TAB	☐
UNANNOUNCED	☐
JUSTIFICATION	
(1 Dec 1954)	
BY	
DISTRIBUTION /	
AVAILABILITY CODES	
DIST	AVAIL AND/OR SPECIAL
A	

Released

DISTRIBUTION STAMP

DTIC ELECTE S D AUG 28 1981 D

DATE ACCESSIONED

UNANNOUNCED

81 6 16 060

DATE RECEIVED IN DTIC

PHOTOGRAPH THIS SHEET AND RETURN TO DTIC-DDA-2

DOCUMENT PROCESSING SHEET

DTIC FORM OCT 79 70A

MASSACHUSETTS INSTITUTE OF TECHNOLOGY
DEPARTMENT OF ELECTRICAL ENGINEERING
HIGH VOLTAGE RESEARCH LABORATORY

FEASIBILITY OF COMPACT 4 MEV ELECTROSTATIC X-RAY SOURCE
STUDIES OF COMPRESSED GAS AND HIGH VACUUM INSULATION
RADIOGRAPHIC PROPERTIES OF X-RAYS IN THE 2 TO 6 MEV RANGE

SUPPLEMENTARY FINAL REPORT

for the period June, 1952 through June, 1954

to the

OFFICE OF ORDNANCE RESEARCH

ON

CONTRACT DA-19-020-ORD-2023

DECEMBER 1, 1954

NOTE: This form is to be executed to show proposed distribution, and forwarded in triplicate to the Chief of Ordnance for prior approval of all distributions. Proposed distribution to agencies or individuals whose official interest in the report is not obvious must be justified by explanatory statements on the back of this form.

BINDING AREA FORM NO. ORDBE-342L. (Rev.) 2 Sept. 1947 BINDING AREA

COPIES PREPARED 10

WATERTOWN ARSENAL
TECHNICAL REPORT DISTRIBUTION

EXTRA COPIES REMAINING

REPORT NO. 142/58-8 TITLE: M. I. T. DA...2023
Supp. Final Rpt. 6/52 - 6/54

TO:	NO. OF COPIES	DATE OCO APPROVAL	DATE SENT	TO:	NO. OF COPIES	DATE OCO APPROVAL	DATE SENT
WATERTOWN ARSENAL-ORDBE				OTHER:			
Laboratory File	1						
~~Author:~~ C. Hastings	1	#2					
OFFICE, CHIEF OF ORDNANCE							
ORDIR-Artillery							
ORDIM-Ammunition							
ORDIT-Automotive							
ORDIS-Small Arms							
ORDTB-Res. & Materials							
ORDTM-Ammunition Dev.							
ORDTR-Artillery Dev.							
ORDTS-Small Arms Dev.							
ORDTT-Tank Automotive							
ORDTU-Rocket Dev.							
ORDTX-Executive							
ORDTX-AR - Executive Library	1						
ORDNANCE DEPARTMENT AGENCIES							
ORDBA-Frankford Arsenal							
ORDBB-Picatinny Arsenal							
ORDBC-Rock Island Arsenal							
ORDBD-Springfield Armory							
ORDBF-Watervliet Arsenal							
ORDBG-Aberdeen Prov. Ground							
ORDJR-Raritan Arsenal							
ORDMX-Detroit Arsenal							

APPROVING AUTHORITY:
Ltr.:
Date:
From:

SUPPLEMENTARY FINAL REPORT

to the

OFFICE OF ORDNANCE RESEARCH

on

CONTRACT DA-19-020-ORD-2023

by the

MASSACHUSETTS INSTITUTE OF TECHNOLOGY

This supplementary report describes the feasibility and the performance characteristics of a four million volt Van de Graaff electrostatic accelerator especially suitable for the continuous and pulsed radiography of heavy metal sections, and applicable to other scientific and medical purposes. Engineering and scientific studies on the properties of compressed gas and vacuum for the insulation of high constant voltages, as well as on other factors influencing the design of such a compact supervoltage radiographic unit, are also summarized.

The final report, submitted in July 1954, covered primarily the experimental studies of the "Radiographic Properties Of X-rays In The Two- To Six- Million Volt Range". A reprint of a recent paper of this title published in the Bulletin of the American Society for Testing Materials is included herein for completeness.

All of the reported work was performed at the Massachusetts Institute of Technology during the two year period beginning June 1952.

December 1, 1954

High Voltage Research Laboratory
Department of Electrical Engineering
Massachusetts Institute of Technology

SUPPLEMENTARY REPORT TO THE OFFICE OF ORDNANCE RESEARCH ON CONTRACT DA-19-020-ORD-2023

Objectives of Engineering and Scientific Studies

In addition to the experimental investigation of the radiographic properties of X rays in the two to six million volt range, an important objective of the work supported at Massachusetts Institute of Technology by the Office of Ordnance Research, was the examination of the feasibility and of the principal performance characteristics of a compact radiographic unit operating at four million volts. A further purpose was to support the fundamental and engineering studies on the insulation of high voltages in vacuum and in compressed gas, on the application of such insulation to the acceleration of electrons to high energy, on the techniques of producing and maintaining high vacua, and on other factors which affect the design of particle accelerators.

This supplement to the final report submitted in July 1954 summarizes the principal results of these additional studies.

Feasibility of a 4 Mev Van de Graaff Accelerator for X-radiography

It was concluded that the ability to insulate high steady potentials in compressed gases and to apply them to the acceleration of electrons in high vacuum, along with associated techniques, had reached the level where the design and prototype production of a compact source of four million volt X rays with high X-ray intensity was both feasible and attractive. This conclusion was based on a background of research and engineering experience in Van de Graaff accelerators extending over many years, but was supplemented in an important way by the additional studies summarized herein on compressed gas and on vacuum insulation. This

statement of feasibility was also based on detailed consideration of an actual four million volt electrostatic accelerator design and on an examination of some of the principal problems which it would present.

CONTINUOUS RADIOGRAPHIC CHARACTERISTICS OF 4 MEV RADIOGRAPHY UNIT

The performance characteristics of such a 4 Mev electrostatic accelerator as a continuous X-radiation source may be summarized as follows:

Operating voltage - 4 million volts, constant potential.

Voltage range - operation at controllable steady voltages in the range from 1 to 4 million volts.

Target current - 250 microamperes.

Current range - controllable from 1 to 250 microamperes.

Maximum X-ray Output - 600 roentgens per minute measured on axis of electron beam at 100 cm from target.

Inherent filtration - equivalent to 10 mm of lead but derived mainly from the 6 mm thick gold target.

Target spot size - 1 mm or less in diameter with magnetic focussing.

Radiographic speed - on type A Eastman Kodak industrial film and standard developing technique, with a 100 cm target-to-film distance the approximate exposure times to give a film density of 1 are:

Steel thickness	Exposure time in seconds
2	0.4
4	1.6
6	6.5
8	28
10	120
12	480

Other radiographic characteristics of this 4 Mev radiation can be determined from the appended paper "Radiographic Properties Of X-rays In The Two- To Six- Million Volt Range".

PULSED CHARACTERISTICS OF 4 MEV RADIOGRAPHIC UNIT

Of scientific and research interest is the high pulsed radiation output which is inherently available from the electrostatic accelerator. The pulsing is usually accomplished by biasing the cathode to cutoff and removing this bias by a positive voltage pulse of the desired length. For high outputs in single microsecond pulses it would probably be preferable to produce a localized discharge at the cathode. Either single or repeated pulses can be produced; the pulsing circuit is mounted within the high voltage terminal and may be triggered by an external light beam.

The X-ray output per pulse is related to the capacitance of the high voltage terminal and the permissible voltage drop during the pulse. For the 4 Mev radiographic unit, about 25 microcoulombs would be delivered to the target during a voltage drop of 0.5 Mev. Thus a single 1 microsecond pulse would deliver a dose of 1r at a distance of 100 cm from the target.

This unusually high dose rate per pulse together with the almost ideal pulsing control obtainable in Van de Graaff accelerators may be valuable for special purposes in high speed radiography.

PHYSICAL CHARACTERISTICS OF 4 MEV RADIOGRAPHIC UNIT

Much of the attention on the four million volt accelerator design was concerned with the physical arrangements needed to maintain reliable yet compact 4 Mev insulation on both terminal and tube, with the solution of the cantilever column problem, and with the development of a

sealed-off acceleration tube.

Figure 1 shows the principal features of the tentatively proposed 4 Mev radiographic X-ray source. Capable of vertical or horizontal mounting on floor or truck, it is contained in a steel pressure tank 54" in diameter and 8' 6" long. The insulating gas would be a mixture of CO_2 and N_2 with a 10% addition of SF_6 to a total gauge pressure of about 400 p.s.i. The insulating length of the acceleration tube and of the column which supports the terminal is 72". This length is determined primarily by the acceleration tube requirements.

The total electric power requirements of this 4 Mev X-ray unit at full load is about 5 kw of 3 phase conventional electric power. The estimated overall electrical efficiency--electron power on the target over total input power--is 20%. The total gross weight of this X ray unit, exclusive of mounting but including the lead shielding around the target, is 7500 pounds. Details of the column design, analysis of the stress in the supporting column when in horizontal position, and details of the acceleration tube design, are included in the appendixed studies.

SUMMARY OF SCIENTIFIC AND ENGINEERING STUDIES

The following investigations were completed during the course of the Office of Ordnance contract both for their general value in the field of particle accelerators and for their bearing on the feasibility of a 4 Mev radiographic unit. Several of these, as noted, resulted in master or doctoral theses completed in the Department of Electrical Engineering at Massachusetts Institute of Technology.

(1) "Electronegative Gas Insulation for Van de Graaff Generators", Sanborn F. Philp, 1953 thesis for M.S. degree in Electrical Engineering, M.I.T.

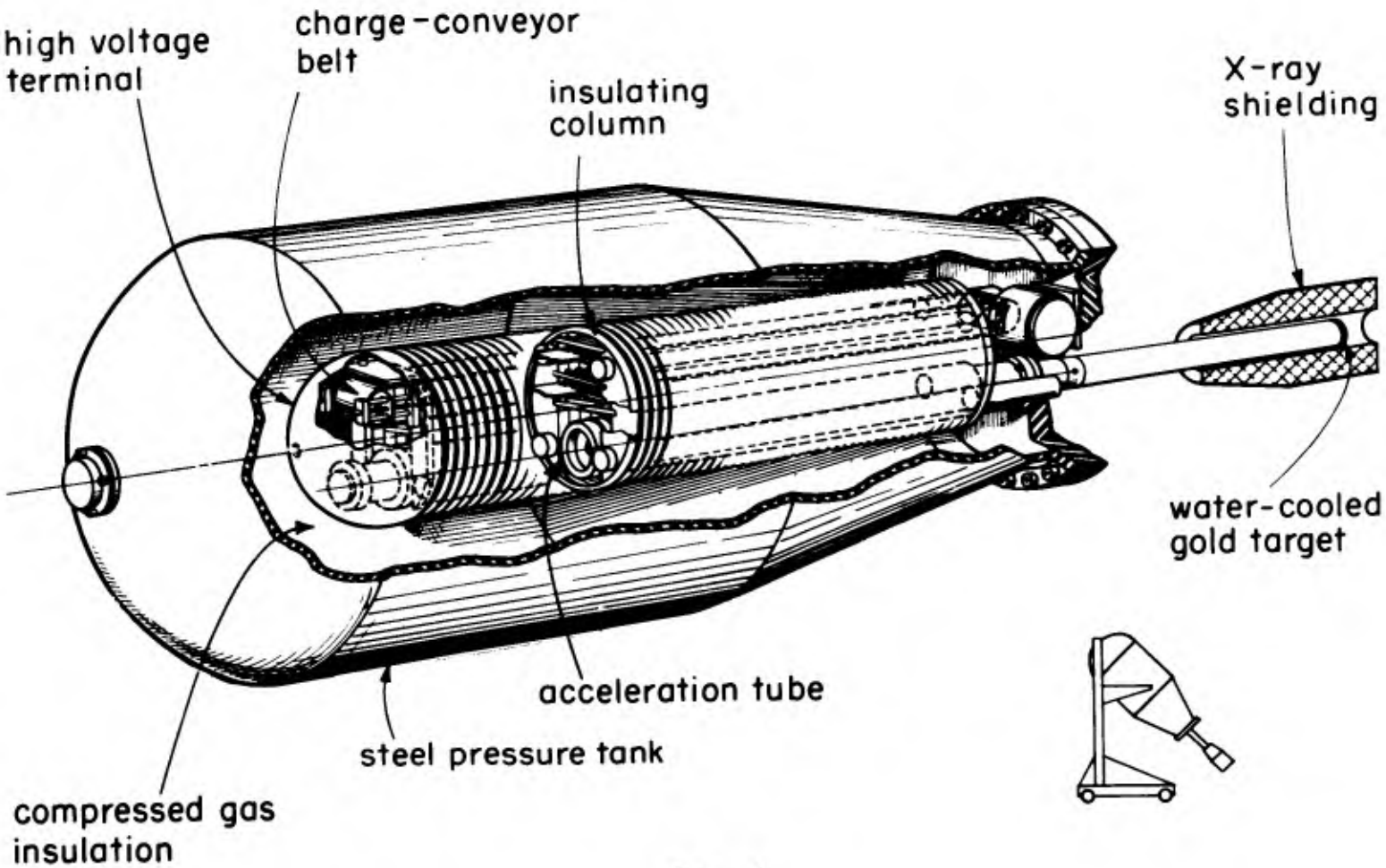

FIG 1

PROPOSED 4 MEGAVOLT GENERATOR DESIGN

(2) "Electrical Processes in High Voltage Acceleration Tubes", Ge Yao Chu, 1953 thesis for Doctor of Science degree in Electrical Engineering, M.I.T.

(3) "Some Calculations Pertaining to the Mechanical Design of Insulating Columns for "Van de Graaff" Generators", R. W. Cloud, 1953.

(4) "Absorption of Gases and Polyvinylacetate Vapors by Evaporated Barium", R. W. Cloud and S. Philp, 1953.

(5) "Adhesives for a Self Supporting Column", R. W. Cloud, 1953.

ELECTRONEGATIVE GAS INSULATION FOR VAN DE GRAAFF GENERATORS.

A summary of a report by Sanborn F. Philp submitted as a M.S. thesis in the Department of Electrical Engineering, Massachusetts Institute of Technology in 1953.

ABSTRACT

Pure sulphur hexafluoride and a mixture of nitrogen and carbon dioxide are compared in a series of experiments involving total voltages up to 3×10^6 volts and gas pressures up to 400 p.s.i. in N_2 and CO_2. Various electrodes were utilized producing both uniform and highly non-uniform fields within the tank of a Van de Graaff electrostatic generator.

It is found that SF_6 is markedly superior to the N_2 and CO_2 mixture only when small electrodes are involved or, in the case of large electrodes, only for pressures below 100 to 150 p.s.i. Conduction currents through the gas are smaller in SF_6, but approach the N_2 and CO_2 values at high pressures.

While no distinct polarity effect is found in N_2 and CO_2, a definite polarity difference is shown in SF_6; higher voltages are obtained when the smaller electrode is positive.

2 MILLION VOLT TEST FACILITIES

As a particle accelerator, the Van de Graaff generator produces a homogeneous beam, closely determined in energy, by passing charged particles from the high voltage terminal to ground in an evacuated tube. Such a procedure requires, however that a potential corresponding to the total particle energy must be insulated by the high voltage terminal. In the modern Van de Graaff accelerator this is accomplished by enclosing the machine in a pressure vessel and insulating the terminal-to-tank gap with compressed gas. Such a pressure insulated machine was utilized for the experiments reported here. These generators are gaining wide use today and are described in many places[1], so a description will not be given here except to state the following specifications:

Terminal diameter	15 inches
Pressure tank inside diameter	30 inches
Column length	24 inches

The terminal is a polished stainless steel spinning mounted on an aluminum base plate. The equipotential planes making up the column are of aluminum (figure 2) and the pressure tank is steel, the inside surface is ground smooth and painted with clear glyptol varnish. This machine is run routinely as a two million volt X-ray generator, but for these experiments the acceleration tube was removed.

ELECTRODE ARRANGEMENTS

Three different stainless steel electrodes; a 6 inch diameter Rogowski electrode[2], a 2 1/2 inch diameter sphere, and a 3/4 inch diameter sphere, were used as grounded electrodes facing the cylindrical part of the high voltage terminal at gaps ranging from 1/4 to 2 1/2 inches.

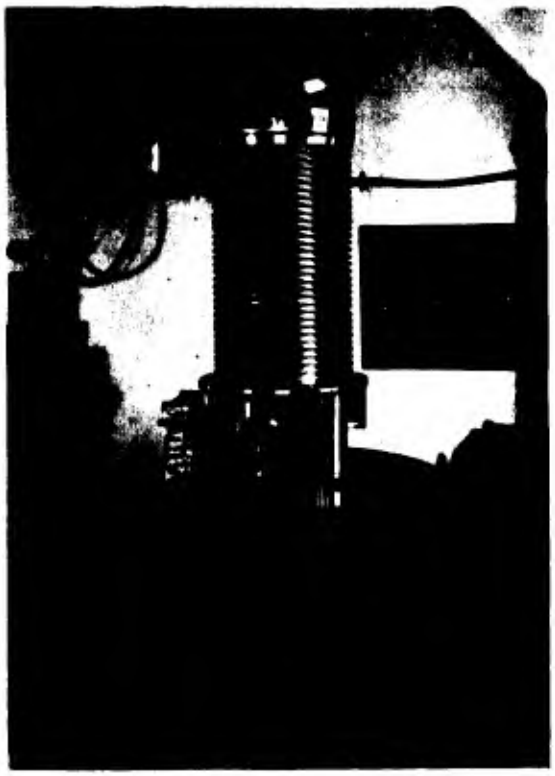

2 MILLION VOLT GENERATOR FIGURE 2

HIGH VOLTAGE TERMINAL FIGURE 3

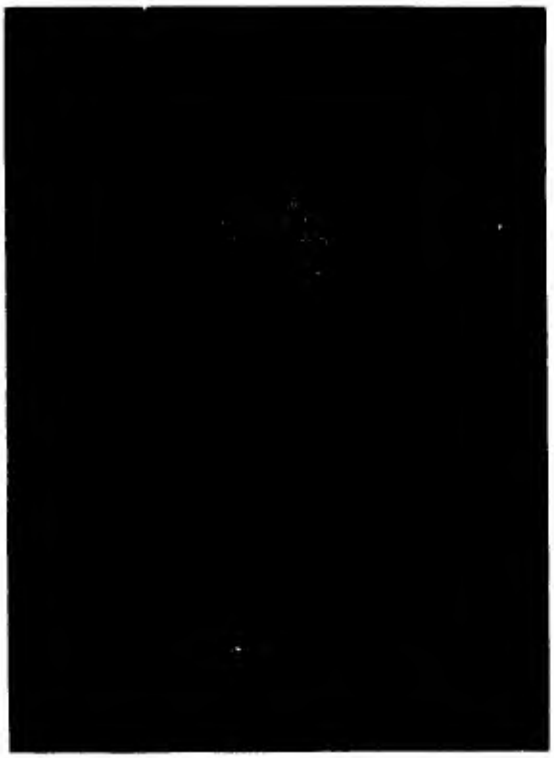

ROGOWSKI ELECTRODE FIGURE 4

$2\frac{1}{2}$" SPHERE FIGURE 5

The experiments were performed for both positive and negative terminal potentials. Currents to the grounded electrode as a function of terminal potential and the number of sparks in a given interval of time were measured. With the Rogowski electrode withdrawn against the tank wall, the full terminal-to-tank gap is available and terminal-to-tank current and sparking rate may be measured.

CRITERION FOR BREAKDOWN

The scattering of breakdown data is considerable at pressures more than a few atmospheres and spacings more than an inch or so. It has become common practice to describe maximum voltage in terms of a certain number of sparks in a given time interval. While this is an arbitrary procedure, it is necessary in order to obtain a practically useful value for the "maximum voltage." For the purpose of these experiments, the criterion used by Kusko[3] of no sparks in three minutes or less than three sparks in nine minutes has been adopted as the definition of maximum voltage.

RELATIVE DIELECTRIC STRENGTH OF SF_6 AND N_2 - CO_2 MIXTURES

Previous work with electronegative gaseous compounds[3] has revealed that under certain conditions their dielectric strength may be several times that of air, N_2, or CO_2 at the same pressure. This general conclusion is borne out by the present investigations. The superiority of SF_6 over a mixture of N_2 and CO_2 (equal parts by volume) is most marked for the case of electrodes with small surface area. For the 3/4 inch sphere the SF_6 maximum voltage at any given pressure and gap is about three times the N_2 and CO_2 value. The superiority of SF_6 diminishes steadily, however, with increasing electrode size, and increasing gap. Since SF_6 must be used somewhat below its saturation

pressure (330 p.s.i. at 20°C), the less condensible gases may overtake much of its dielectric performance at still higher pressures. Thus the maximum terminal-to-tank voltage insulated in SF_6 is only about 20%, higher than the N_2 and CO_2 value at 400 p.s.i.g.

POLARITY EFFECTS IN SF_6 AND N_2 - CO_2 MIXTURES

There is no well defined polarity effect in N_2 and CO_2. In SF_6 there is a polarity effect apparently obeying the law that higher voltages are possible in an arrangement which makes the electrode of smallest size positive.

EFFECT OF ELECTRODE SURFACE GRADIENT

It is interesting to consider the values of maximum gradients on the electrode surface which correspond to the observed maximum voltages. On the assumption of zero space charge, that is, Poisson's equation is valid throughout the gap, the gradient on the electrode surface may be calculated. The terminal has a diameter of 15 inches and the Rogowski electrode a diameter of 5 inches, so with gaps not exceeding 2 1/2 inches it is probably adequate to regard the Rogowski electrode-terminal situation as a uniform field. In this case the gradient on the Rogowski electrode is equal to the potential difference between electrode and terminal divided by the electrode - terminal gap. In the case of the spherical electrodes, the gradient is a maximum at the point on the sphere intercepted by a line passing through the center of the sphere and the center of the terminal. Furthermore, it is justifiable to regard the terminal as an infinite plane with respect to the 2 1/2 inch and 3/4 inch spheres. With these assumptions, calculation of the gradient on the sphere is not difficult, the simplest procedure probably being that of a series of successive images[4].

The maximum gradient as a function of pressure for the three different electrodes is presented in figures 11 and 12. The outstanding feature of these plots is that in N_2 and CO_2 the maximum gradients on the 3/4 inch sphere are twice those on the Rogowski electrode. In SF_6 with the terminal negative the maximum gradients on the 3/4 inch sphere are three times those on the Rogowski electrode.

ELECTRODE DAMAGE

Each spark which passes between the electrodes produces a small mark resembling a pin-point burn in stainless steel and resembling a small sputtering crater in aluminum. This process is described as "conditioning". It is generally agreed that conditioning improves the maximum voltage between stainless steel electrodes and does not damage them from a voltage performance standpoint. The photographs, figures 3, 4, and 5, show the electrodes as they appeared at the end of the experiments. Though the electrode damage appears very severe in these photographs, the breakdown voltage was actually increased by these sparks involving relatively small amounts of stored energy.

PREBREAKDOWN CURRENT AS A FUNCTION OF VOLTAGE, POLARITY, AND ELECTRODE CONFIGURATION

It is of importance to know not only the permissable voltage which can be insulated reliably in gases at high pressure but also to have an appreciation of the magnitude of the prebreakdown current which traverses the inter-electrode gap.

These currents are primarily caused by ionization by electron collision, the Townsend alpha process, though at high gas pressures it is now known they are increased by photoelectric ionization in the gas and by several cathode emission processes including photoelectric and high field emission.[5] It would therefore be anticipated that the stable

prebreakdown currents would be higher when the electrode of smallest radius of curvature was negative. It would also be expected that the prebreakdown currents for a given voltage and electrode system would be less with an electronegative gas such as SF_6. Such gases derive their principal advantage as high voltage dielectrics from their inherent tendency to attach free low-energy electrons, thereby neutralizing their ability to cause further ionization by collisions. These expectations are confirmed and placed on a more quantitative basis by the measurements summarized in the curves below.

Figures 6 and 7 show the breakdown voltage between the terminal and several small grounded electrodes as a function of gas pressure. Figures 8 and 9 show the dependence of breakdown voltage between terminal and tank on both gas pressure and polarity. Figure 10 shows terminal-to-tank current as a function of voltage for both positive and negative terminal.

From this data we conclude that:

(a) The total prebreakdown current is a function of the AREA of the electrode system and may constitute a significant level when the full terminal and tank surfaces are involved.

(b) The prebreakdown current is substantially higher when the electrode of smallest radius of curvature is at NEGATIVE polarity.

(c) For the same voltage and gas-pressure the prebreakdown current is far less in electronegative gases.

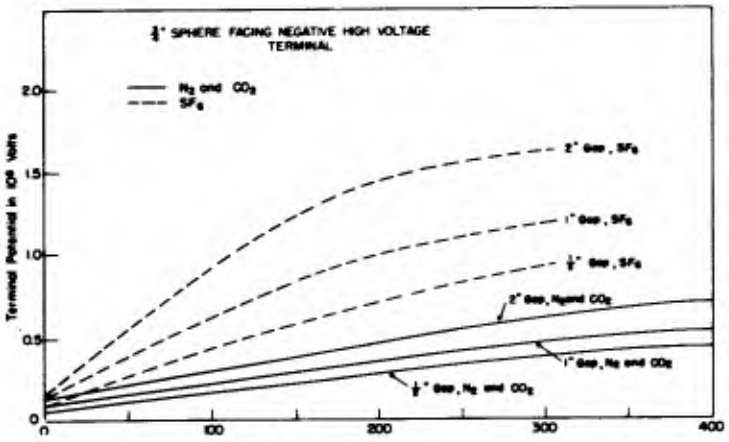

Figure 6

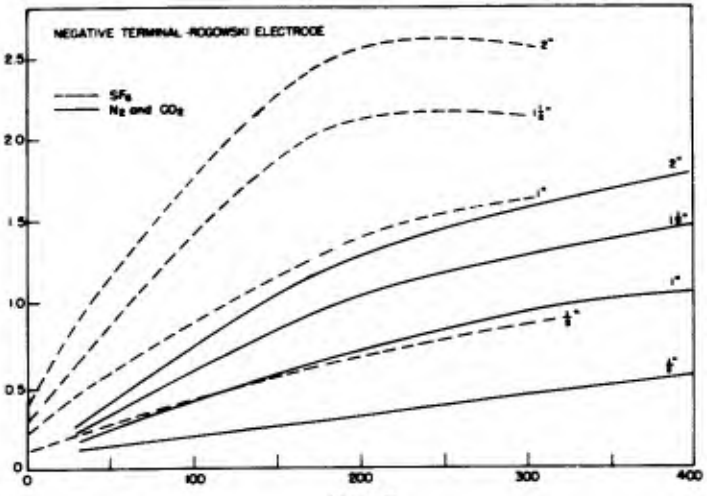

Figure 7

BREAKDOWN VOLTAGE FROM ELECTRODE TO HIGH VOLTAGE TERMINAL

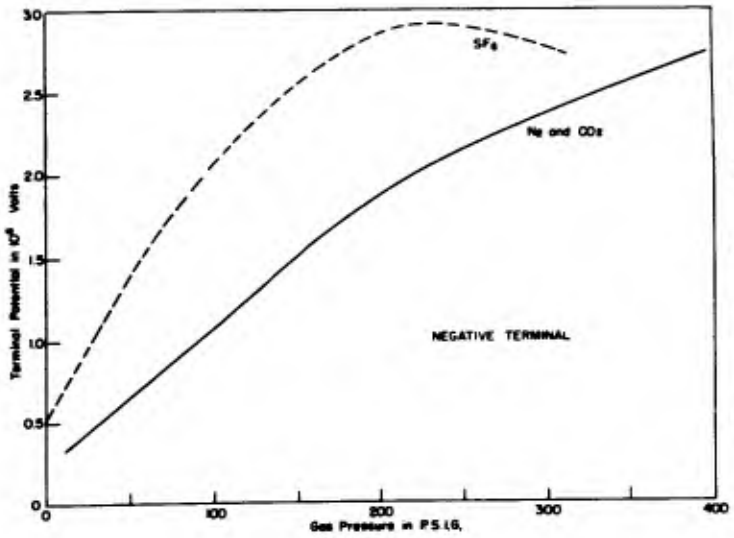

Figure 8

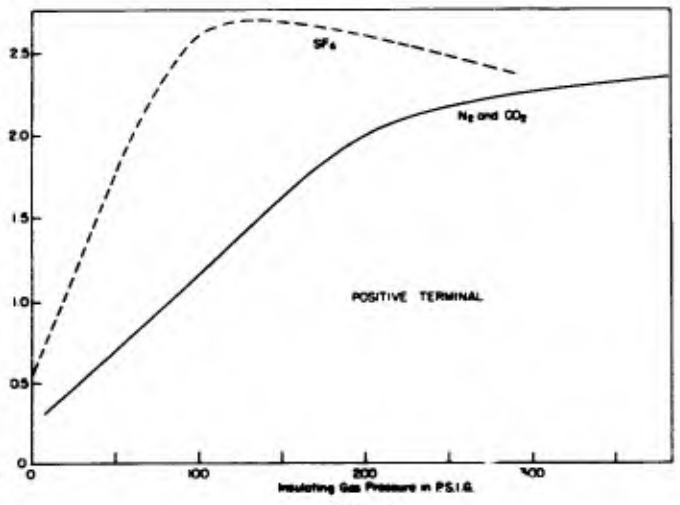

Figure 9

TERMINAL-TO-TANK BREAKDOWN VOLTAGE

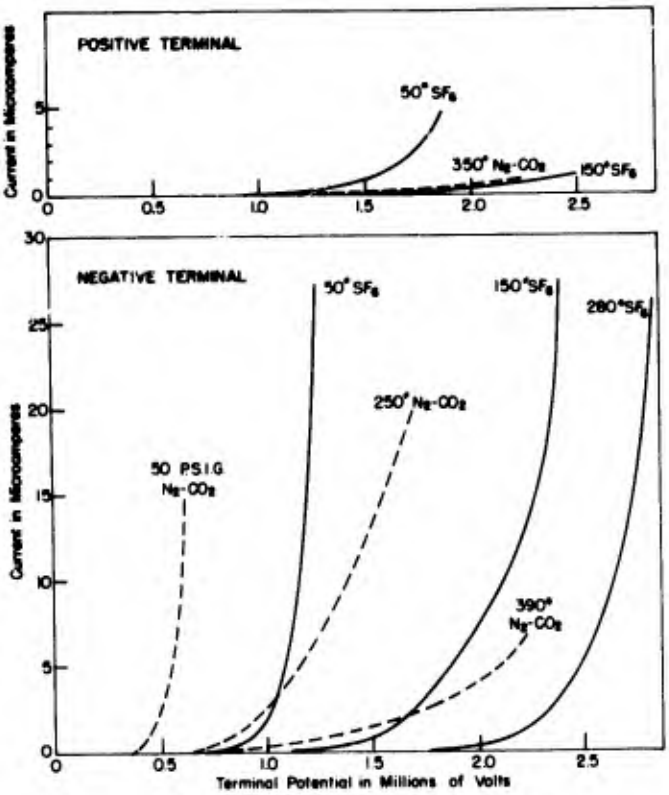

Figure 10. TERMINAL-TO-TANK CURRENT

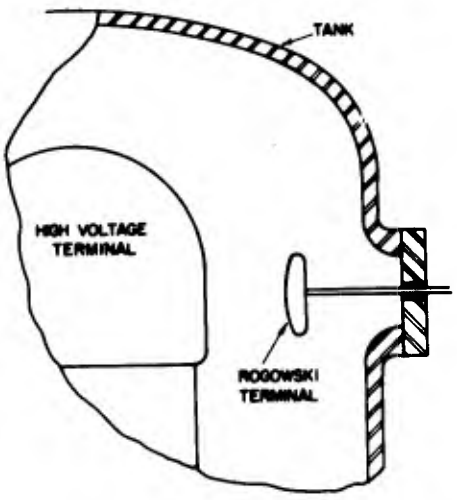

TYPICAL ELECTRODE ARRANGEMENT

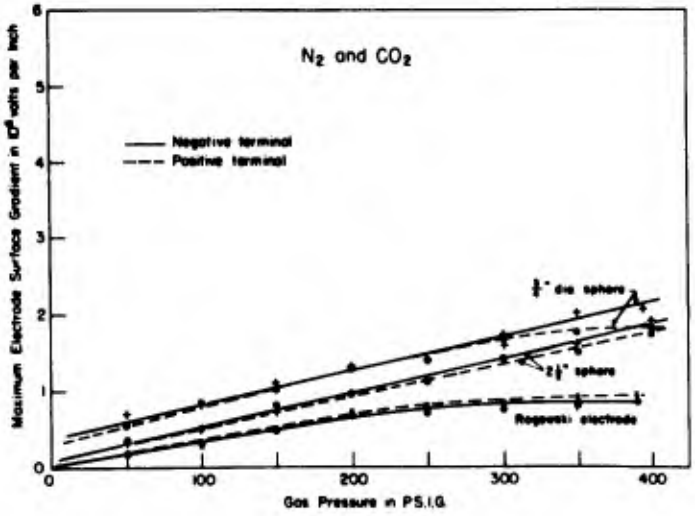

Figure 11

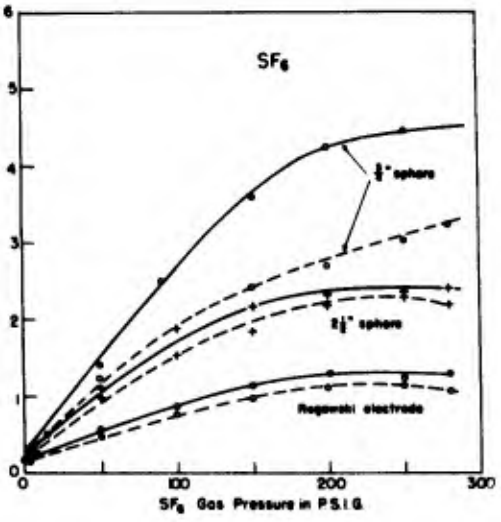

Figure 12

MAXIMUM ELECTRODE GRADIENT FOR TWO INCH TERMINAL-TO-ELECTRODE GAP

FOOTNOTES

1. See, for example, J. G. Trump and R. J. Van de Graaff, A compact pressure insulated electrostatic generator, Phys. Rev., 55, 1160, (1939).

2. W. Rogowski, Archiv fur Elektrotechnik, 12, 1, (1923).

3. A. Kusko, A study of the electrical behavior of gases at high pressures, M.I.T. Doctor's thesis, E.E. Dept., 1951.

4. Dean, Phys. Rev., Dec., 1912, April, 1913.

5. J. G. Trump, R. W. Cloud, J. G. Mann, and E. P. Hanson, Influence of electrodes on d-c breakdown in gases at high pressure, Elec. Eng. 69 #11, 961, Nov., 1950

ELECTRICAL PROCESSES IN HIGH VOLTAGE ACCELERATION TUBES

A summary of a report by Ge Yao Chu submitted as a D. Sc. thesis in the Department of Electrical Engineering, Massachusetts Institute of Technology in 1953

OBJECTIVES OF ACCELERATION TUBE RESEARCH

The tank and terminal diameters of a Van de Graaff accelerator are determined by the breakdown strength of the gas-filled gap between terminal and tank, while the length of the generator is determined primarily by the performance of the acceleration tube. Although the structural column of the generator and the charge-conveying belt as well as the particle-accelerating tube must insulate the full terminal potential, it is the electrical instabilities within the tube which determine the required column length and which impede the attainment of higher energies.

For this reason the study of electrical processes within acceleration tubes and the improvement of tube design are primary research objectives in the effort to produce compact particle accelerators.

Electric breakdown across a single gap between metallic electrodes immersed in high vacuum has been carefully studied in the High Voltage Research Laboratory, particularly for long gaps and high total voltages[1]. Although several of the mechanisms whereby charged particles are released from the electrodes are now understood, the mechanism of vacuum breakdown is not simple and a quantitative theory has not yet been achieved. In the design of improved acceleration tubes which consist of many gaps in series one must rely upon this still incomplete theory of the vacuum breakdown process supported by information on the relative

performance in vacuum of various materials, electrode and insulator configurations, and of prior tubes. To a large extent, this procedure has evolved the present tube design which is capable of accelerating 2 Mev particles in a two-foot length. It is our conviction that further improvements will follow a better understanding of the nature of the electrical processes and instabilities which develop in high voltage vacuum tubes. The work of Ge Yao Chu[2] is the most recent research in the continuing program of this laboratory to elucidate the mechanisms of vacuum breakdown, especially in the complex acceleration tube system.

STRUCTURE OF THE ACCELERATION TUBE

The two million volt electron acceleration tube (Fig. 13) consists of an evacuated cylindrical accelerator structure closed at the high-voltage-terminal and by a cathode containing a hot filament electron source and terminating at the other end in a grounded metal tube extension finally closed by the gold target. The insulating portion of the tube is 24 inches long and is made up of annular glass insulators alternated with aluminum diaphragms - the electrodes. The distance between successive electrodes is usually 3/4 inch which corresponds to the distance between equipotential planes in the compressed-gas-insulated electrostatic generator. Each electrode is connected to an equipotential plane and is thereby maintained at a definite fraction of the terminal potential.

Each electrode is provided with an axial hole to allow the electron beam to traverse the tube. The diameter of this hole may be varied along the tube length. Three such variations, or tapers, were studied: 1) the single taper - hole diameters increasing steadily from the cathode to the anode end. 2) the double taper - hole diameters decreasing steadily from the cathode to some intermediate point in the tube and then steadily in-

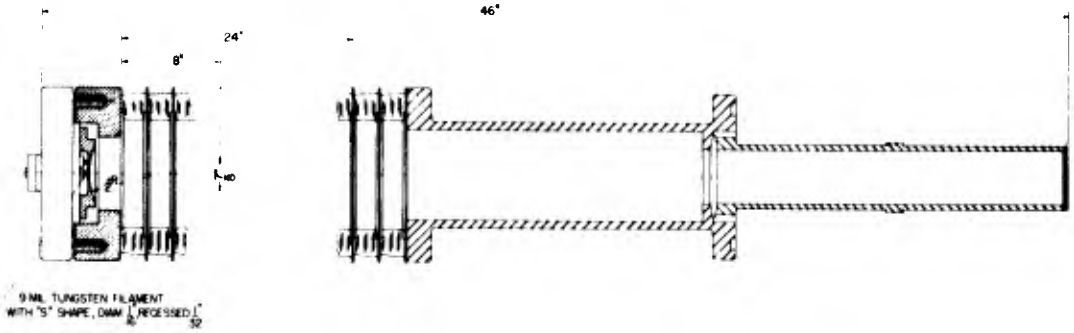

Figure 13

SECTIONAL VIEW OF A TWO-FOOT X-RAY TUBE WITH A POWER FUNCTION FIELD CATHODE GUN

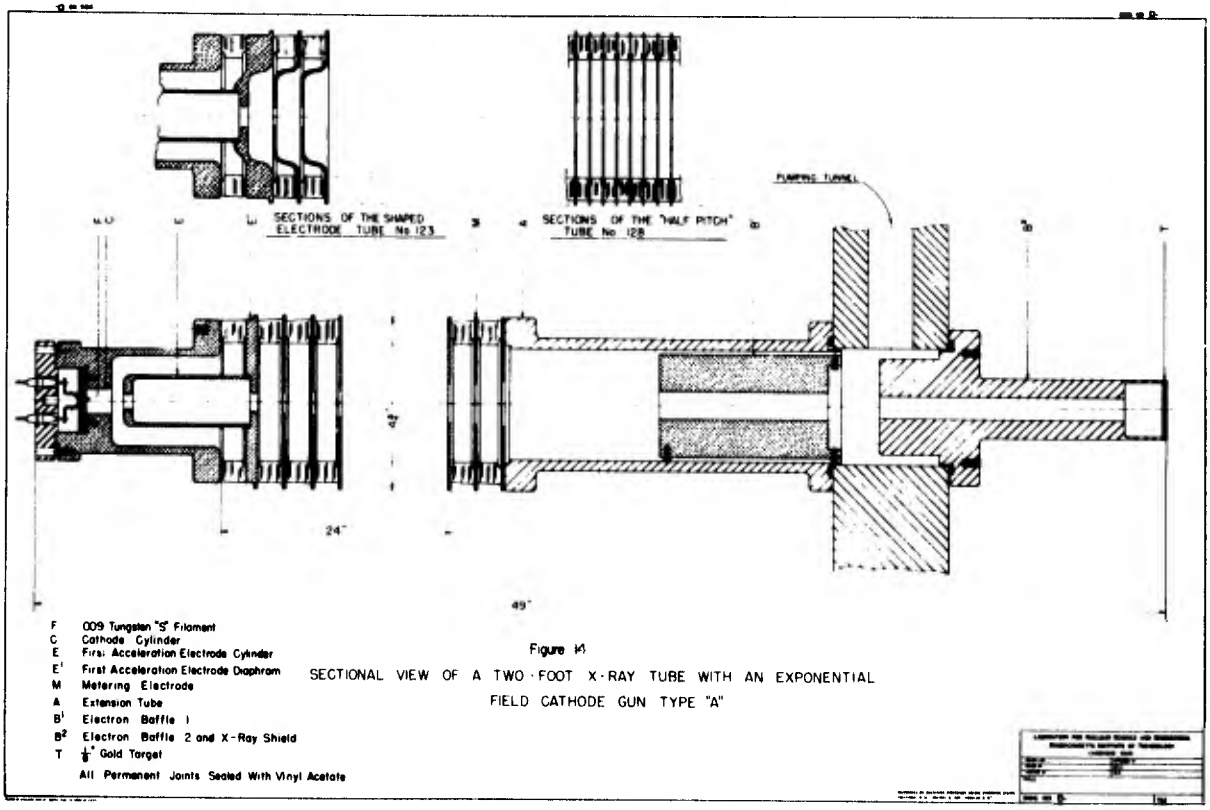

Figure 14

SECTIONAL VIEW OF A TWO-FOOT X-RAY TUBE WITH AN EXPONENTIAL FIELD CATHODE GUN TYPE "A"

creasing toward the target. 3) no taper - all holes of the same diameter. Both flat and shaped electrodes were studied. These together with a "half-pitch" construction are shown in figure 14.

CONDUCTION AND BREAKDOWN

Two distinct forms of electrical instability in acceleration tubes will now be described.

As the generator voltage is increased, at a fairly well defined voltage the acceleration tube will become highly conductive with a sudden disappearance of most or all of the terminal charge and energy. This is called a tube spark or breakdown. Often sufficient gas is released by this discharge to cause the tube to remain conducting until the belt current brought to the terminal is reduced. This spark breakdown produces little x-radiation, the terminal charge does not reach the target. The breakdown voltage often shows dependence upon electrode and insulator contamination, but it is doubtful that there is a conditioning process which will raise the tube breakdown voltage.

At voltages below the breakdown voltage a sudden pulse of charge may pass down the tube. In contrast to the tube spark, this is a transient instability of variable magnitude from which complete recovery follows. Since the terminal voltage may drop from 1 to 10% during this discharge, it is commonly referred to in this laboratory as a kick. The charge flowing during a kick may end up on any of the electrodes or other parts of the tube, but the focussing properties of the tube cause most of the charge to reach the target in almost every case. Penetrating radiation is therefore produced and an analysis of the X-ray quality and quantity per microcoulomb of electrons to the target reveals that a substantial part of the charge in a kick has the full terminal energy.

Within certain limits, the threshold voltage for kicks may be raised by the conditioning process of allowing kicks of limited energy to occur.

The distinction between tube kicks and tube breakdown became further clarified during these investigations. The spark breakdown is now believed to occur along the inside surface of the glass insulator. Thus a spark passes the length of the tube from terminal to ground by passing from electrode to electrode along or very near the inside surface of the glass. This is supported on disassembly of the tube by the vertical spark tracks along the inside of the glass insulators. A tube which has sparked will usually have such marks on every insulator. In contrast, a tube kick is believed to originate at or propagate to the cathode and then pass down through the axial holes in the electrodes producing particles at the anode of full terminal energy.

INFLUENCE OF TAPERED AXIAL HOLES

The breakdown voltage did not vary significantly among the three tubes having the three different tapers, nor was there a noticeable difference between the flat electrode and the shaped electrode tubes. Segments about six inches long of a single taper tube were tested with the part of the tube not under test shorted out. There was no significant difference among the breakdown voltages of the various segments, which seems to indicate that electrode hole size does not play an important part in determining breakdown voltage.

One of the tubes was made of electrodes entirely coated with a 0.0001" thick coating of polyvinyl acetate (Bakelite AYAT). There was no evidence that this treatment raised the breakdown voltage and, in addition, performance of the tube was generally poor due to the large amounts of gas evolved whenever the coated surface was bombarded with

charged particles, as in a kick or spark. The coated-electrode tube was tested because of indisputable evidence that an insulating film on the metal electrodes would significantly raise the voltage and reduce the pre-breakdown current in single gaps in vacuum.

EFFECT OF DEGREE OF VACUUM ON TUBE PERFORMANCE

Arrangement was made to vary the gas pressure in the acceleration tube. A fixed leak was connected into the vacuum system, and the high pressure side of the leak was connected to a flask in which the gas pressure was easily variable, thus providing a variable leak rate. This arrangement makes it possible to introduce various known gases into the tube.

The breakdown voltage was independent of pressure from the highest vacuum obtained up to about 10^{-4} mm. of mercury, at which pressure a glow discharge formed in the tube.

The threshold voltage for tube kicks, on the other hand, increased with increasing pressure until the pressure for glow discharge was reached. This interesting effect which had previously been studied in this laboratory, is displayed in the curves of figure 15. Figure 15 also shows the improvement of the kicking threshold with conditioning. Curves (1), (2), and (3) are for air and represent increasing stages of conditioning. Curves (4) and (5) are for argon. Curve (4) shows that conditioning was taking place during the test.

EFFECT OF NUMBER OF SECTIONS ON TUBE SPARKS

The breakdown strength of a single high vacuum gap has been found to vary approximately as the square root of the gap length. In addition, increase of electrode area reduces the breakdown voltage; the shape and composition of solid insulators in proximity to the gap may also have a

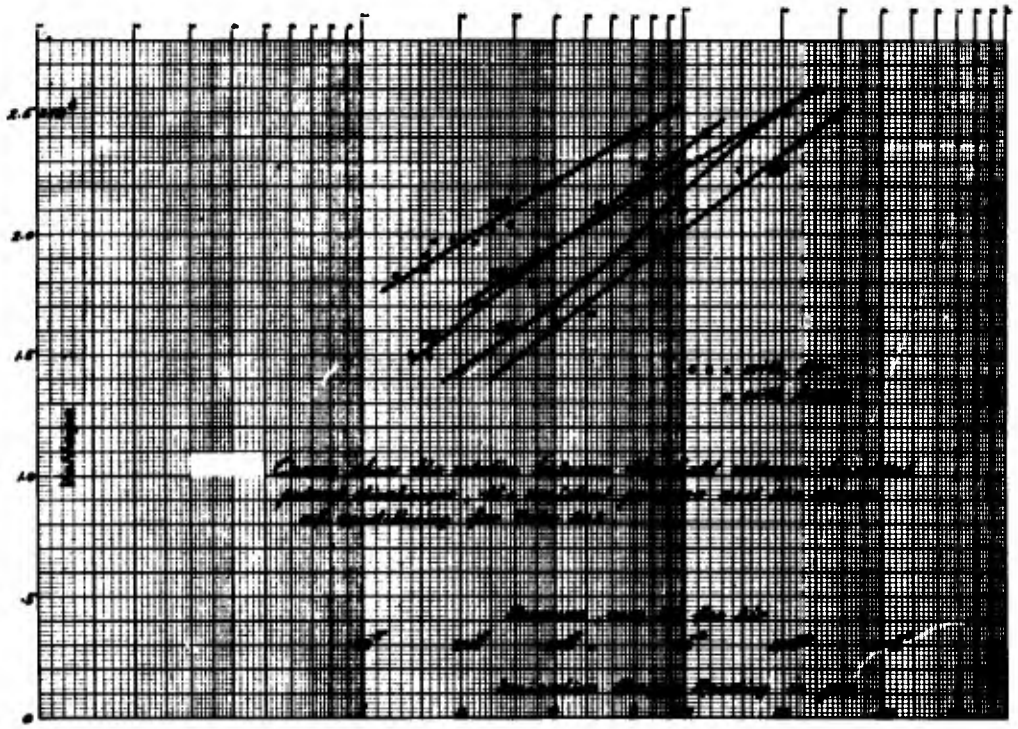

Figure 15
THRESHOLD VOLTAGE FOR TUBE KICKS AS A FUNCTION OF GAS PRESSURE IN TUBE

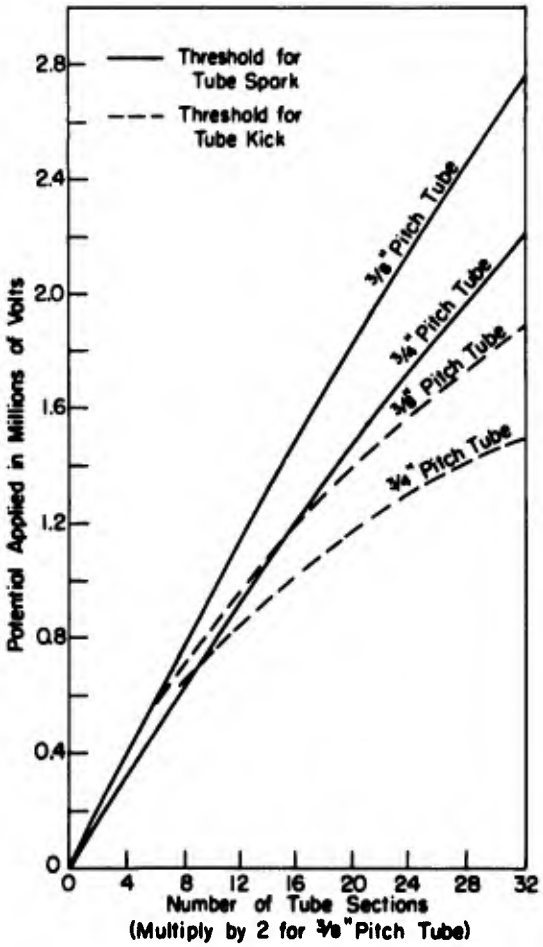

Figure 16
VOLTAGE PERFORMANCE OF ACCELERATION TUBE

dominant influence on the voltage performance[3].

With the total tube length divided by the electrodes into a succession of vacuum gaps connected in series, one might expect the tube breakdown voltage to increase linearly with the number of sections. In the limit, the voltage of such a system could be equal to the single gap strength multiplied by the number of sections in series. By shorting out various lengths of the tube, starting at the grounded end, it was found that the breakdown voltage does increase almost linearly with the number of active sections. (Fig. 16)

Since the single gap strength is proportional to the square root of the gap length, while the strength of the tube is approximately the sum of the individual gap strengths, it should be possible to raise the breakdown voltage of a tube of given length by increasing the number of sections. To test this idea, a "half-pitch" tube was constructed and tested. The construction of the generator column made it necessary to leave alternate electrodes of the half-pitch tube floating, i. e., not connected to the column. The half-pitch construction is illustrated in figure 14 and the performance of the tube is indicated in figure 16. A maximum voltage of 2.75 million volts was achieved on the half-pitch tube (24 inch length, 3/8 inch between electrodes) compared to 2.2 million volts for the standard 3/4 inch pitch tube. Once again, the breakdown strength varied almost linearly with the number of sections across which voltage was applied.

EFFECT OF NUMBER OF SECTIONS ON TUBE KICKS

The threshold for tube kicks was found to be 1.9 million volts for the half-pitch tube. In order to reach the maximum breakdown voltage with satisfactory and reproducible results it was necessary to introduce addi-

tional gas pressure in the tube to quench the kicks.

The threshold for tube kicks varies approximately as the square root of the number of sections in series for all of the tubes tested. (See Fig. 16) In an attampt to explain this variation with length, it is possible to assume that the kicking threshold is proportional to the product of cathode gradient and total voltage, thus obtaining the necessary half-power law. The evidence showing that tube kicks have the full terminal energy lends some credence to this idea, but is hard to give the formula any firm physical basis. Cranberg has made an attempt in this direction with his "clump" theory.[4]

INVESTIGATION OF THE DE-COUPLING OF TUBE SECTIONS

The glass insulators of a tube are in series, but a path is provided through the axial electrode holes to propagate a disturbance originating in one section throughout the length of the tube. The beam holes thus provide a tunnel which "couples" all of the sections, thus partly vitiating the series strength of the arrangement.

A tube having no central beam hole was built and tested in the two million volt machine. Holes were made in the electrodes for pumping, but no two adjacent electrodes had holes which lined up. This tube had a breakdown strength essentially the same as other tubes of the same length and pitch, but no kicks were observed at any attainable voltage. This is essentially consistent with the proposed mechanism of tube breakdown, moreover, it suggests that by making the central hole in the electrodes as small as possible to approach the condition of de-coupled tube sections, the threshold voltage for tube kicks will be increased. The limitation on the size of the central hole is provided by the electron optics of the tube. A single taper

tube with a small hole running from 3/8 inch dia. at the cathode to 3/4 inch dia. at the anode end was tested, but, unfortunately, the results were somewhat inconclusive.

CATHODE FOCUSSING ARRANGEMENT FOR VAN DE GRAAFF ACCELERATOR TUBES

The cathode structure shown in figure 13 is typical of that used in electron accelerators. It has the virtue of simplicity, but its focussing properties are limited. A cathode focussing arrangement for use in a Van de Graaff accelerator must meet five requirements:

1. A sufficiently small spot size at the target for radiographic or medical purposes.
2. A well collimated beam throughout the length of the tube so that few beam particles will be lost to the electrodes.
3. Both criteria 1 and 2 must be satisfactorily maintained over a wide range of operating voltages.
4. The electric field at the cathode surface should be low compared to that on other electrode surfaces.
5. The structure should be simple to meet the space and power limitations in the terminal of the generator.

The electron gun shown in figure 14 was developed in this laboratory[2] to meet these requirements. It requires only the filament power supply - the focussing potentials are obtained from the current flow in the generator column resistors. The target spot size is 1/8 inch in diameter for a 250 microampere beam, an improvement of at least 50% over the previous design.

The reduction in spot size is a two-fold achievement: The usefulness of the machine for medical and radiographic applications is extended, and the improvement of electron optics within the acceleration tube con-

tributes to tube performance and thus to the performance of the machine as a whole.

CONCLUSION

This work has further clarified the distinction between acceleration tube sparks and kicks. It has shown that the sparking voltage - for a tube of given length and construction - can be increased by further sectionalizing.

The voltage threshold for kicks may be increased by increasing the residual gas pressure to a value close to that at which ionization by electron collision becomes significant. It may also be increased by diminishing the diameter of the axial holes in the electrodes.

An analysis of the electron optics for the electron accelerating kicks has resulted in a design which gives better collimation of the beam. This permits smaller axial holes in the electrode system and produces a smaller target spot for radiography.

FOOTNOTES

1. J. G. Trump and R. J. Van de Graaff, Phys. Rev., 55, 1160, (1939)
H. W. Anderson, Elec. Eng., 54, 1315 (1935)
J. G. Trump and R. J. Van de Graaff, Journ. Appl. Phys., 18 #3, 327 (1947)
H. C. Bourne, Jr., Sc.D. Thesis, Elec. Eng., M.I.T. (1952)
Webster, Van de Graaff, and Trump, Journ. Appl. Phys., 23 #2, 264 (1952)
W. B. Green, Sc.M. Thesis, Elec. Eng., M.I.T. (1952)

2. Ge Yao Chu, Sc.D. Thesis, Elec. Eng., M.I.T. (1953)

3. P. H. Gleichauf, Journ. Appl. Phys., 22 #5, 535 (1950)
Journ. Appl. Phys., 22 #6, 766 (1951)

4. L. Cranberg. Univ. Calif., Los Alamos Sci. Lab. Rep. (1952)

SOME CALCULATIONS PERTAINING TO THE MECHANICAL DESIGN OF INSULATING COLUMNS FOR "VAN DE GRAAFF" GENERATORS*

The insulators in the columns of "Van de Graaff" generators are sectionalized at regular and frequent intervals with metal planes to permit subdivision of the high terminal voltages. For horizontal operation these sectionalized insulators must be capable of supporting in cantilever their own weight and that of the terminal and associated equipment. Glass is the usual insulator because of its high electrical breakdown strength and ease of cementing. A fairly strong bond can be made between the glass and the metal plates with a cold setting adhesive of the epoxy type.

The belt and tube are also insulators which must be sectionalized and are therefore included in the column structure. To a large extent they determine the general size of the column and the layout of the insulators. A cross-sectional view of a typical column is shown in figure 17, while that of the proposed 4 million volt generator column is shown in figure 18.

For strength calculations these designs, especially that of figure 18, may be represented as two beams, each of which has a column of insulators at its top and bottom edges (see figure 19). These two columns of insulators are tied together by the metal plates. This report presents calculations for the mechanical strength and deflection of such beams. In addition to developing general equations, particular results are given for the columns of figures 17 and 18. Although the calculations are usually applied to obtain stresses and deflections due to

---

*This is a summary of an M.I.T. laboratory report presented by R. W. Cloud in November 1952.

gravitational forces acting on horizontal columns, they can also be used to estimate the stiffness of vertical columns of similar design, and the sideways stiffness of horizontal columns.

METHOD OF CALCULATION

The sectionalized beam sketched in figure 19 is considered as two insulator columns, shown in figure 20, each of which take 1/2 of the loading and in addition have bending moments M_1, M_2, etc and longitudinal forces supplied by the metal tie pieces. The moments are in a direction to help reduce the deflection of the beam, and the longitudinal forces are in a direction which produces tension in the top column and compression in the bottom. Since the moments are quite frequent and regularly spaced their summation is approximated by an integral.

The calculations presented here are for beams which have both ends of each insulator column mounted on hingetype supports which transmit tensile, compressive, and shear forces but permit no bending moment at the ends of the columns. Calculations for other end conditions can be found by changing the constants of integration in the solution, equation 13. Such calculations were made for the case where the insulators are rigidly attached to a heavy metal plate at the base, but are omitted from this report since this condition results in a very high fiber stress in the bottom insulators. An estimation of the fiber stress in this case is given by the results tabulated under rigid base for the column of figure 17.

SUMMARY OF CALCULATED EQUATIONS

The maximum deflection,

$$y_{max} = \frac{L^3}{2EIA^2} \left(P + \frac{W}{2}\right) \tag{1}$$

P is the load at the end of the beam.

W is the total of the evenly distributed load.

L is the length of the beam.

E and I are the modulus of elasticity and moment of inertia of the area of one glass beam.

A is the stiffness constant of the connecting metal plates,

$$A = \sqrt{\frac{6Lnei}{gEI}} \tag{2}$$

n is the number of connecting metal plates.

g is the length of the metal plates or the spacing between insulators.

e and i are the modulus of elasticity and moment of inertia of the connecting metal plates.

The maximum bending moment is at the middle of the beam and is produced by W only;

$$M_m = \frac{WL}{2A^2} \left(1 - \frac{1}{\cosh 1/2A}\right) \tag{3}$$

The tensile force in the middle of the top glass beam is

$$T_m = \frac{L}{g}\left\{\frac{P}{2} + \frac{W}{2} - W\left[.375 - \frac{1}{A^2}\left(1 - \frac{1}{\cosh 1/2\ A}\right)\right]\right\} \tag{4}$$

The fiber stress at the mid-section of the column is

$$S_m = \frac{Tm}{area} + \frac{Mm}{I/r} \tag{5}$$

The bending moment at the base is zero, but the tensile force is

$$T_b = \frac{L}{g}\left(P + \frac{W}{2}\right) \tag{6}$$

DISCUSSION OF RESULTS

These calculations have shown that rigid supports for the insulating columns produce high stresses and are therefor undesirable. The deflection with hinged supports at the ends is generally acceptable even with relatively weak tie plates which alone prevent the column from sagging. Adding other hinged connectors in the column breaks it mechanically into a number of shorter columns and further reduces the fiber stress. The design proposed for the 4 million volt generator has 2 such mechanical links which break the column into 3 lengths each 2 feet long. This markedly reduces the fiber stress and also allows the divisions to be easily handled.

With hinged supports a beam is shown by equation 14 to deflect to a straight sided parallogram as far as the terminal load is concerned, but the distributed load adds a non-linear deflection. Since the maximum bending moment occurs at the middle of the column and the maximum tensile loading occurs at the base, the point of maximum fiber stress will be between the base and the middle. In the column of figure 17 hinged at the base the maximum bending moment predominates and the maximum stress is near the middle, but in the column of figure 18 the opposite is true and the maximum stress is near the bottom insulator. It would be possible to grade the size of the insulators to match the stress, but the added complexity didn't seem desirable in these cases.

The stiffness of the connecting plates will be determined by the permissable deflection. In these examples the hoop adds to the stiffness of the connecting plates. The sideways stiffness is almost entirely due to the hoops. The stiffness of the metal plates could only be roughly approximated for the column of figure 17, but the deflection calculated agrees well with measured values.

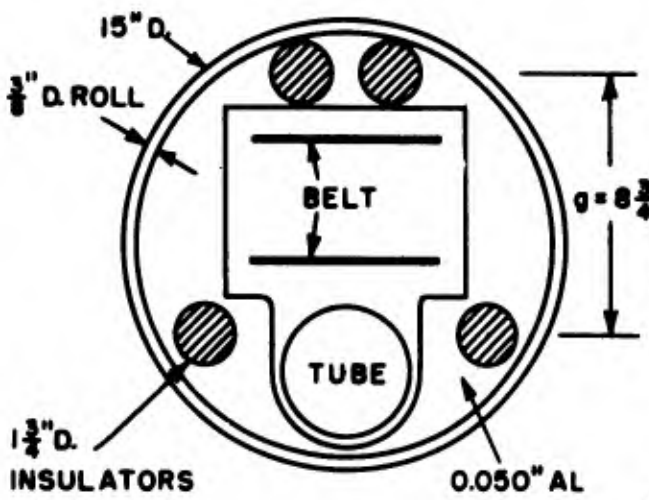

Fig. 17. Cross Section of 33" long column of 44 sections.
Terminal Weight = 100#
Column Weight = 100#

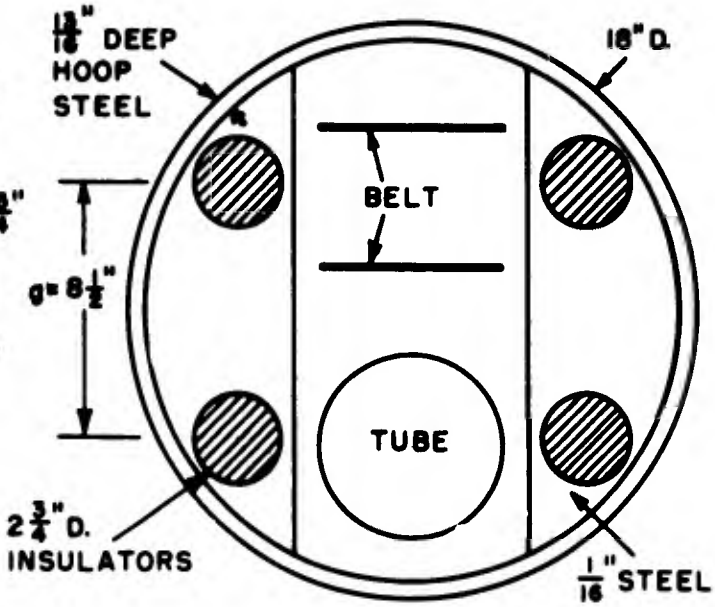

Fig.18 Cross Section of 6' long column to consist of 3 divisions with hinged connectors between. Each division is 25" long with 20 sections.
Weight each division is 150#
Terminal weight is 100#

SUMMARY OF CALCULATIONS FOR COLUMNS OF FIGURES 17 AND 18

	Figure 17		Figure 18
	Rigid Base	Hinged at Base	
Maximum deflection, inches	.070	.193	.041
Deflection for 100# added terminal load	.051	.13	.013
Maximum shear per sq. in.	21	21	23
Tension per sq. in. at base	44	117	291
Bending moment stress at base	1470	0	0
Max. fiber stress at base	1510	117	291
Tension per sq. in. at middle of bottom division		57	264
Bending moment stress at middle of bottom division		157	21
Max. fiber stress at middle of bottom division		214	285

DETAILED CALCULATIONS*

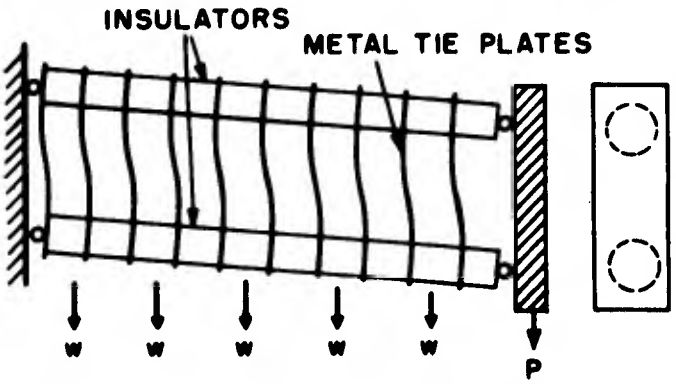

FIG. 19 EXAGERATED SKETCH OF BEAM

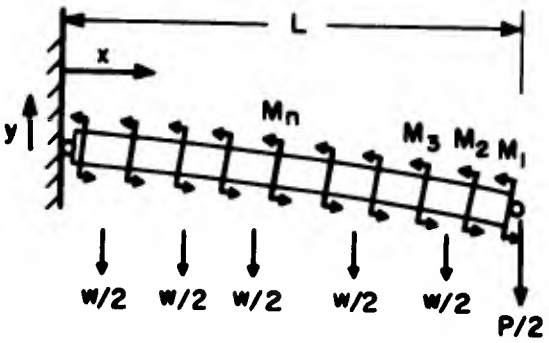

FIG. 20 BEAM EQUIVALENT TO ONE GLASS COLUMN

To determine M_1, M_2,$-M_n$, the moments produced by the metal tie piece:

The equations for the n^{th} metal tie piece as a beam are

$$ei \frac{ds}{dr} = \int M dr = \int [M_n + F(g - r)] \, dr$$

$$\text{and } F = \frac{2M_n}{g} \qquad (7)$$

With the choice of axii shown in figure 21 the solution of these equations give:

$$S = \frac{M_n}{ei} \left(\frac{r^2}{2} - \frac{r^3}{3g}\right)$$

and $M_n = \frac{6ei\, S_{max}}{g^2}$ where S_{max} is the deflection for $r = g$.

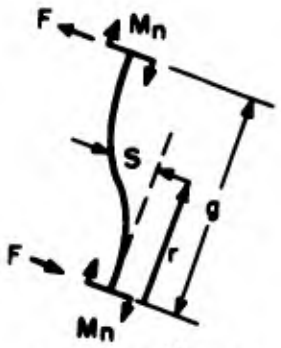

FIG. 21 n^{th} TIE PLATE AS A BEAM

From figure 22

S_{max} = -g x slope of insulating column

$= -g \left(\frac{dy}{dx}\right)$ where $\frac{dy}{dx}$ refers to the beam of fig. 20.

So $M_n = \frac{-6ei}{g} \frac{dy}{dx}$ (8)

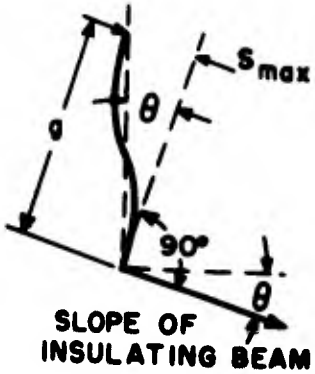

FIG. 22 GEOMETRY OF n^{th} TIE PLATE

* Many symbols are defined on page 23.

EQUATIONS OF THE BEAM OF FIGURE 20

Moment at any section,

$$M = -\frac{P(L-x)}{2} - \frac{w}{2}\frac{(L-x)^2}{2} - \sum_{\substack{n=1 \\ n \text{ value at } x}} 6\,\frac{ei}{g}\left(\frac{dy}{dx_n}\right) \qquad (9)$$

Since the metal spacers will be regularly and closely spaced, the moments may be approximated by a continuous moment change per unit length. Then if $\frac{n\,ei}{L}$ represents the value of ei per unit length,

$$M = -P/2\,(L-x) - w/4\,(L-x)^2 - 6\int_x^L \frac{n\,ei}{Lg}\,\frac{dy}{dx}\,dx \qquad (10)$$

This equation reduces to:

$$\frac{d^3y}{dz^3} - A^2\,\frac{dy}{dz} = B + D\,(1-z), \qquad (11)$$

$$\text{when } z = x/L;\ A^2 = \frac{6nL}{g}\,\frac{ei}{EI};\ B = \frac{PL^3}{2EI};\ D = \frac{WL^3}{2EI}\ . \qquad (12)$$

The solution of the above is:

$$y = C_1 + C_2\,e^{Az} + C_3\,e^{-Az} + \frac{D}{2A^2}\,z^2 - \frac{(B+D)}{A^2}\,z \qquad (13)$$

If the base of the beam has hinged supports, the constants of integration are found by substituting the values:

$y = o$ when $z = o$

$\frac{d^2y}{dz^2} = o$ when $z = o$ and when $z = 1$.

This makes the solution:

$$y = -\frac{L^3}{2A^2EI}\left\{Pz + W\left[z - \frac{z^2}{2} - \frac{1}{A^2}\left(1 - \frac{\sinh Az - \sinh A\,(z-1)}{\sinh A}\right)\right]\right\} \qquad (14)$$

The maximum deflection is at $z = 1$, so

$$y_{max} = -\frac{L^3}{2A^2EI}\left(P + \frac{W}{2}\right)\ . \qquad (1)$$

The moment anywhere is

$$M = EI \frac{d^2y}{dx^2}.$$

Thus:

$$M = \frac{WL}{2A^2}\left[1 - \frac{\sinh Az - \sinh A(z-1)}{\sinh A}\right]. \qquad (15)$$

The maximum moment occurs when $\frac{d^3y}{dz^3} = o$ which makes $z = 1/2$,

and $M_{max} = \frac{WL}{2A^2}\left(1 - \frac{1}{\cosh 1/2A}\right)$. (3)

The tensile and compression forces are found by referring

to equations (7) and (8)

$$T = \sum_{\substack{n=1 \\ n \text{ value at } x}} F = \frac{12\, n\, ei}{g^2 L} \int_x^L \frac{dy}{dx}\, dx = \frac{2EIA^2}{gL^2}\,(y_L - y_x) \qquad (16)$$

or $$T = \frac{L}{g}\left\{P + \frac{W}{2} - Pz - W\left[z - \frac{z^2}{2} - \frac{1}{A^2}\left(1 - \frac{\sinh Az - \sinh A(z-1)}{\sinh A}\right)\right]\right\}. \qquad (17)$$

When $z = o$ this reduces to

$$T_o = -L/g\ (P + W/2) \qquad (18)$$

When $z = 1/2$ or at the middle.

$$T_m = -L/g\left\{P/2 + W/2 - W\left[3/8 - \frac{1}{A^2}\left(1 - \frac{1}{\cosh 1/2\, A}\right)\right]\right\} \quad (4)$$

ABSORPTION OF GASES AND POLYVINYLACETATE VAPORS BY EVAPORATED BARIUM

by

R. W. Cloud and S. Philp

M.I.T., December 1953

This report summarizes the results obtained with a first design of an absorption vacuum pump using evaporated barium as the absorbing medium. This is called a pump since it was designed to replace the diffusion pump and cold trap and has valves which permit the system to be opened without exposing the barium. The barium can be evaporated as needed with an electric heater and if need be the pump can be opened to replace the barium supply. This has been a good system for experimental work and the information obtained is directly applicable to the design of a sealed-off high energy acceleration tube.

DISCUSSION OF RESULTS

This barium pump has never approached the hundreds of liters per second obtained with titanium absorption pumps by Professor Ray Herb at Wisconsin. Ray Herb's high speeds were obtained with continuous evaporation of titanium which gave a continuously fresh surface for absorption. However, with this first barium vaporizer design, continuous evaporation was not advantageous since the gas given off by the ceramic form (Norton R-139) on which the heater was wound kept the equilibrium pressure at about 2×10^{-4}mm when the barium was heated to the 750°C which produced evaporation. The surface formed by the evaporation of one gram of barium (one hour at 750°C) over an area of about 500 sq cm in conjunction with activation of the gas by a Philips gage maintained the system at an equilibrium pressure of 7×10^{-6}mm as read by the Knudsen gage, while

the Philips gage equilibrium is 3×10^{-7}mm since the ionizable gases are preferentially absorbed. It is thought that the pumping speed of about 1 liter per second for permanent gases is limited by the rate of diffusion of the gas into the volume of the barium. The barium absorbs considerable quantities of gases before the pumping speed is reduced to 1/2 value (20 mm L of air). Therefore, in pumping suitable systems, one layer of barium will act as a pump for some weeks before evaporation of a new layer of barium is required.

Nitrogen, oxygen, and hydrogen were absorbed by the barium without being activated by an ionization source, except for a small fraction of a percent which is probably impurity. Helium (and presumably other noble gases) was not absorbed by the barium until activated by the Philips gage and then the pumping speed is low. Air was absorbed by the barium alone except for 1% which is about the amount of argon to be found in air. The vinylacetate vapors were not absorbed by the barium until activated by the Philips gage or until decomposed by a hot filament. The pumping speed is low for this activated polyvinylacetate vapor, and is not limited by the rate of ionization of the Philips gage, since the speed was the same whether either one of two gages or both were on together. The speed is probably limited by the effective area of barium exposed.

Attempts to increase the effective barium area by flashing in a 5 mm pressure of argon were frustrated by arcing of the heater; the 80 volts was enough to cause an arc at this pressure when any barium was emitted.

APPARATUS

The pump was designed with a relatively large supply of barium (45 grams) which can be evaporated to the walls as needed by heating with an electric heater. Since the evaporation temperature was only 750°C the

barium was placed in an iron crucible surrounded by a 300 watt molybdenum heater coil. The vacuum packed barium as received from the Kemet Company was opened and melted into the crucible in an atmosphere of helium. Exposure of this crucible to air caused a surface film which got deeper with time but was not objectionable after one day and could be scraped off easily after a week's exposure.

The base of the pump consisted of two sylphon valves with lead seats permitting the system to be opened with the barium chamber closed. A Welch mechanical fore pump was used to rough out the system before opening to the barium. During this test the system being pumped consisted of a pipe connecting the barium chamber to a Knudsen gage and a second Philips gage, a leak and measuring manometer for admitting bottled gases, and during the tests of polyvinlyacetate an HK-54 ion gage and a 500 ml flask containing six loosely rolled cylinders of aluminum foil with a total area of 300 sq in coated on one surface with polyvinlyacetate AYAT. The system contained 16 polyvinylacetate and 5 Armstrong A-6 joints and two pipe threads sealed with red glyptal but no rubber gasketed joints.

ABSORPTION OF PERMANENT GASES

The pumping speed with the Philips gage and the barium was constant until over 7 mmL of air is absorbed and varies for the different gases as follows:

Gas	Air	N_2	O_2	H_2	He
Speed in L/sec	.85	1.05	1.7	4	.06

This speed is the ratio of the gas admitted to the equilibrium pressure as read by the Knudsen gage and was usually measured at a pressure of about 5×10^{-5}mm. The pumping speed for air diminished with gas absorbed as follows:

Total air absorbed (mmL)	.2	2.5	6.7	11.6	15	20
Speed for air in L/sec	.85	.83	.82	.6	.46	.4
Ultimate vacuum by Philips	$2x10^{-7}$	$3x10^{-7}$			$4x10^{-6}$	$4x10^{-6}$
Ultimate vacuum by Knudsen	$7x10^{-6}$	$7x10^{-6}$			$1\ 1/2x10^{-5}$	$1\ 1/2 \times 10^{-5}$

It is essential to have the Philips gage on to completely absorb any of the gases. Without the Philips gage 1.1% of the air admitted is not absorbed which is equal, within experimental error, to the .96% of argon in air; .3% of the oxygen, .1% of the nitrogen, .05% of the hydrogen and all of the helium admitted were not absorbed. These could be the percentages of noble gases present as impurities in these bottled gases. The polyvinylacetate and other organic vapors coming from the system joints would also not be absorbed, but this background was negligably small in this test ($5x10^{-9}$ mmL/sec was not absorbed 5 days after evacuation).

The Philips gage alone had a speed of .09 L/sec for air.

The use of the Philips gage on top of the barium chamber, with its neck removed, gives 13% higher pumping speed for air than is obtained with the use of the Philips gage mounted at the other side of the system by the Knudsen gage. With both gages on, the increase in pumping speed is only about 10% over that with the getter Philips gage. Apparently the pumping speed for air is limited by something other than the ionization rate of the gages; this may be the diffusion rate into the barium. However, there is a change in speed with Philips gage voltage which amounts to an increase of about 30% in speed for air when the voltage is raised from 2300 volts to 5000 volts. The speed of pumping helium is increased by 300% for a similar change in Philips gage voltage. The pumping speed figures given in the above tables are for a Philips gage voltage of about 2300 volts.

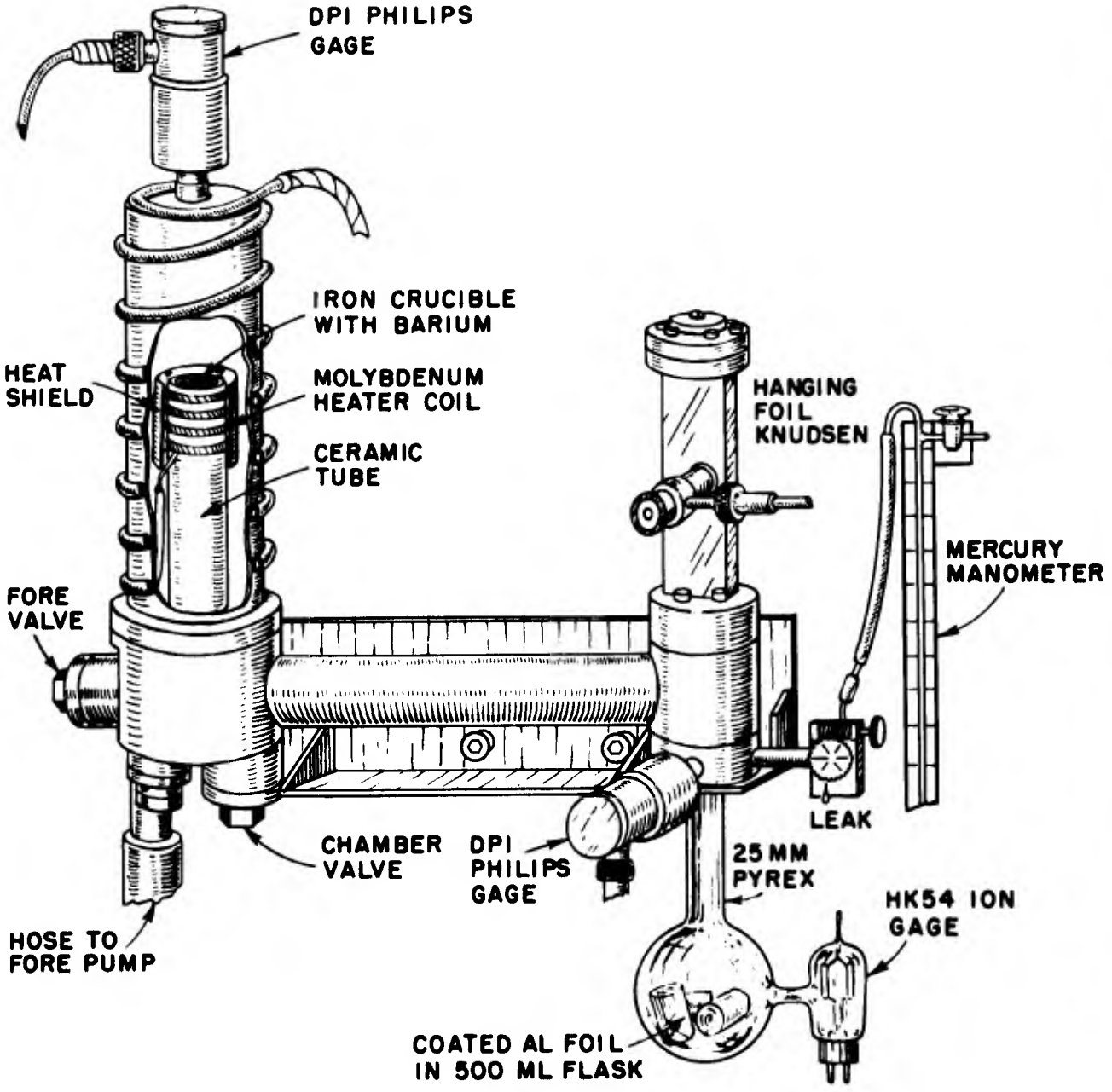
DPI PHILIPS GAGE
IRON CRUCIBLE WITH BARIUM
HEAT SHIELD
MOLYBDENUM HEATER COIL
CERAMIC TUBE
HANGING FOIL KNUDSEN
MERCURY MANOMETER
FORE VALVE
LEAK
CHAMBER VALVE
DPI PHILIPS GAGE
25 MM PYREX
HK54 ION GAGE
HOSE TO FORE PUMP
COATED AL FOIL IN 500 ML FLASK

FIG 23

ABSORPTION OF POLYVINYLACETATE VAPORS

A study was made of the gas from a sample consisting of 300 sq in of 1 1/2 mil thick aluminum foil coated on one side with almost .001 inch thickness of polyvinylacetate AYAT: the quantity of gas emitted, its absorption by barium and a Philips gage (singly and together), as well as the effect of a glowing filament were studied.

This study confirms previous results which showed that the quantity of gas which comes from polyvinylacetate is small, especially after pumping for several days. However, practically none of this gas was absorbed by barium alone.

The polyvinylacetate vapors were decomposed by a glowing filament. In these tests, decomposition by the filament of an HK-54 tube, with the other electrodes floating, increased the quantity of gas emitted by a factor of 30. These decomposed gases were readily absorbed by barium, so that, with the barium available, the pressure rise is somewhat less with the filament on than with it off, and the equilibrium pressure with the combination barium plus Philips gage is not changed by heating the filament. In fact, the combination of an HK-54 filament and barium was sufficient to maintain a constant pressure of 7×10^{-5} mm after 91 hours evacuation and 2×10^{-5} after 188 hours. The action of the filament seems to be limiting and a filament of much larger area in conjunction with barium to absorb the decomposed gas might make a suitable absorber.

A Philips gage or ionization gage in addition to the barium permits the polyvinylacetate vapors to be absorbed, although the pumping speed is low. There is no absorption by either the barium or Philips gage when used singly. The Philips gage does not decompose the gas in the same way as the hot filament since the pressure rise with a Philips gage on is the

same as with it off whereas the hot filament causes a large multiplication of the gas emitted. In this test, the absorption limitation was not in the Philips gage since the equilibrium pressure as read by the Knudsen was the same whether the gage next to the barium, or the one some distance away, or both are on. Since the limitation is not in the amount of ionization by the Philips gage, an increase in pumping speed could be expected by increasing the barium area.

The quantitative results are summarized in the following table in which the figures listed are from Knudsen gage readings unless otherwise headed.

Hours after evac.	Pressure rise, mmL/sec				Equilibrium Pressure with ba. & P.gage.	
	system alone	with ba.	with filament	with ba. & fil.	Knudsen	P.gage
21	1.9×10^{-6}	1×10^{-6}			2×10^{-5}mm	
49	5×10^{-7}	5×10^{-7}	1.2×10^{-5}	3×10^{-7}		
68	3×10^{-7}	2.7×10^{-7}	9.5×10^{-6}	1.8×10^{-7}	$1\ 1/2\times10^{-5}$	5×10^{-7}
91	1.8×10^{-7}	1.9×10^{-7}	5.8×10^{-6}	1.3×10^{-7}	$1\ 1/4\times10^{-5}$	3×10^{-7}
188	1.2×10^{-7}	1.5×10^{-8}	3.8×10^{-6}	1.3×10^{-8}	8×10^{-6}	2×10^{-7}
212	8×10^{-8}	2.4×10^{-8}			1×10^{-5}	1×10^{-7}

It is interesting to note that, except for the last reading, the gas evolution diminishes by a factor of two every 24 hours while the equilibrium pressure does not diminish proportionally. After the above absorption test for polyvinylacetate this barium surface was still capable of absorbing nitrogen at 1.1 L/sec speed.

The gas becomes low in easily ionizable constituents after the Philips gage has been on for some time, and the ratio of Knudsen reading to Philips gage reading increases from 1.7 to 10. (readings of 2nd Philips gage were used since it is mounted near the Knudsen). This ratio was checked at

about 1 for air in earlier tests.

The increase in pressure rise with a heated filament was studied versus filament temperature. For temperatures above 800 to 900 degrees centigrade, the rate of decomposition of gas was unaffected by the temperature of the filament.

Polyvinylacetate surfaces conditioned by several days of pumping so that they evolved only small quantities of gas were exposed to atmospheres of nitrogen and oxygen and after reevacuation did not require further conditioning except to remove a superficial film of nitrogen or oxygen. However, after exposure to carbon-dioxide for one hour at atmospheric pressure, the gas evolved was greater than when the sample was first evacuated. This gas continues to come out for several days and is still being emitted at the rate of 1.2×10^{-7} mmL/sec after 68 hours evacuation. The emitted gas is thought to be mainly carbon dioxide since it is mostly absorbed by barium alone.

SUGGESTIONS FOR FURTHER DESIGN

There were two faults with the barium heater: gas evolution was too great from the ceramic heater support, and the 80 volt heater could not be operated in a few mm pressure of argon because the heater voltage was too great. These would both be solved by heating the barium through the wall of the vacuum chamber, using an external heater. This might permit continuous evaporation with much increased pumping speed. A larger barium area will also increase the pumping speed. This can be obtained by larger physical size, by evaporation in argon, or maybe by some proper internal baffles.

ADHESIVES FOR A SELF SUPPORTING COLUMN

To determine the suitability of adhesives for the column assembly, tests have been made on the long time tensile, shear strength and cold flow properties of several adhesives for glass-to-metal joints. Solvent type adhesives cannot be used because there is no means for escape of the solvent. Thermoplastic and thermosetting adhesives must be used with caution because of strains due to the difference in thermal expansion coefficients of the glass and metal. Adhesives which chemically polymerize at room temperature are most suitable. Epon VI (manufactured by Armstrong Products Company and Shell Oil Company) is such an adhesive and of the many materials tried gives the strongest glass to metal joint.

Our measurements of the strength of seals between glass and aluminum made with Epon VI, cured with 6% accelerator A at room temperature, are tabulated in Tables 1, 2, 3, 4, and the graph of Fig. 26. The joint thickness is usually about .004" but the few joints made with less than .001" thickness showed the same strength. The tensile tests indicate a long-time strength of about 1200 lb. per square inch, even at slightly elevated temperatures and a short time, or shock strength, of 3800 lb. per square inch. Tests also indicate a tensile strength limitation in the glass, and tempered glass is to be obtained if possible. Glass is used because of its good electrical properties and ease of cementing. A shear load of 1100 lbs. per square inch causes only .0001" creep in 2 months at 100°F and no breakage in 6 months at 136°F.

The cold shock test is an indication of internal strains which arise from differences in expansion coefficient of the joined materials

and cause the glass to break. The choice of sample size was arbitrary but is a rather severe test since the samples have a large sealing area. The breakage is at the same temperature as when other adhesives were used which left no strains at room temperature. This test plus past experience indicates that the glass to steel or aluminum joints are satisfactory for the column but the exposed end glasses should be sealed to a low expansion metal.

Robert W. Cloud

June 1953

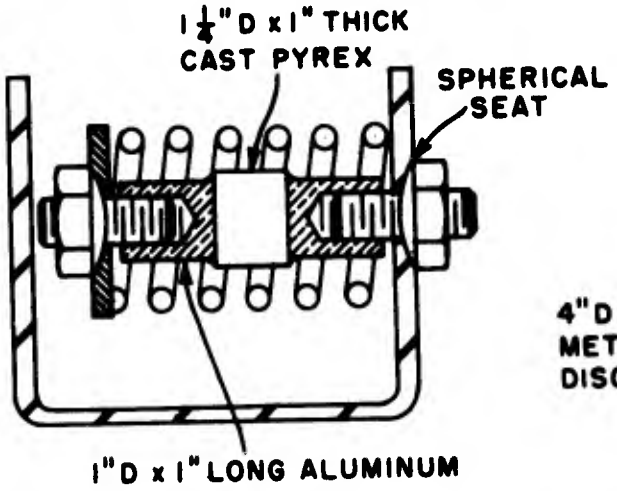

Arrangement used for testing the tensile strength of adhesive joints.

Fig.24

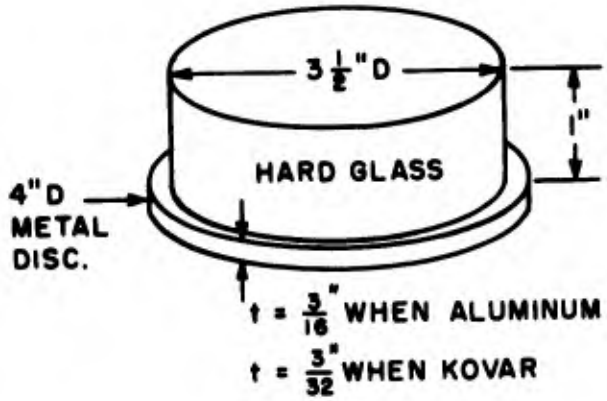

Sample for cold-shock test.

Fig. 25

TABLE 1

Short Time Tensile Strength of Joints Made With Epon VI using 6% accelerator A.

Load Increase of 100#/sec.

2 - 1" diameter aluminum pieces butt joined to each side of 1 1/4" diameter glass broke in joint at 3800 #/^{2}in.

2 - 2" diameter steel pieces butt joined to each side of 1 7/8" diameter glass broke in glass at 2500#/^{2}in.

TABLE 11

Long Time Tensile Strength of 2 - 1" diameter aluminum pieces butt-joined to each side of a 1 1/4" diameter glass (see Fig.24). The break is always in the joint.

Adhesive	Loading #/^{2}in	Time at 100° F	Time at 140° F
Epon VI	1500	2 hrs. to break	
"	1300	3 hrs. to break	
"	1200	3 months plus	5 1/2 months and still unbroken
"	1050	3 months plus	3 months to break
"	900	3 months plus	2 months to break
Epon VI thinned with 6% xylene	1050	1 1/2 months plus	1 1/2 days to break
Epon VI thinned with 6% xylene	900	1 1/2 hrs. to break (joint not complete to edge at one spot)	
Armstrong C2	1050	7 hrs. to break	
"	900	1 1/2 hrs. to break	
"	750	1 1/2 months plus	5 1/2 months and still unbroken

TABLE III

Epon VI 1"dia. aluminum to aluminum	1500	1 to 3 hrs. to break	
"	1200	1 1/2 months plus	1 1/2 months to break

TABLE IV

Cold Shock Test (see Fig.25)

With aluminum, no breaking when dunked in 10° c water
" " 2 out of 4 break when dunked in 0° c water for 5 min.
With Kovar no breakage when dunked in -30° c alcohol.
" " 1 out of 3 break when dunked in -47° c alcohol.

FIG 26. CREEP DURING SHEAR LOADING
EPON VI JOINING GLASS TO ALUMINUM
7 DAY CURE AT ROOM TEMPERATURE

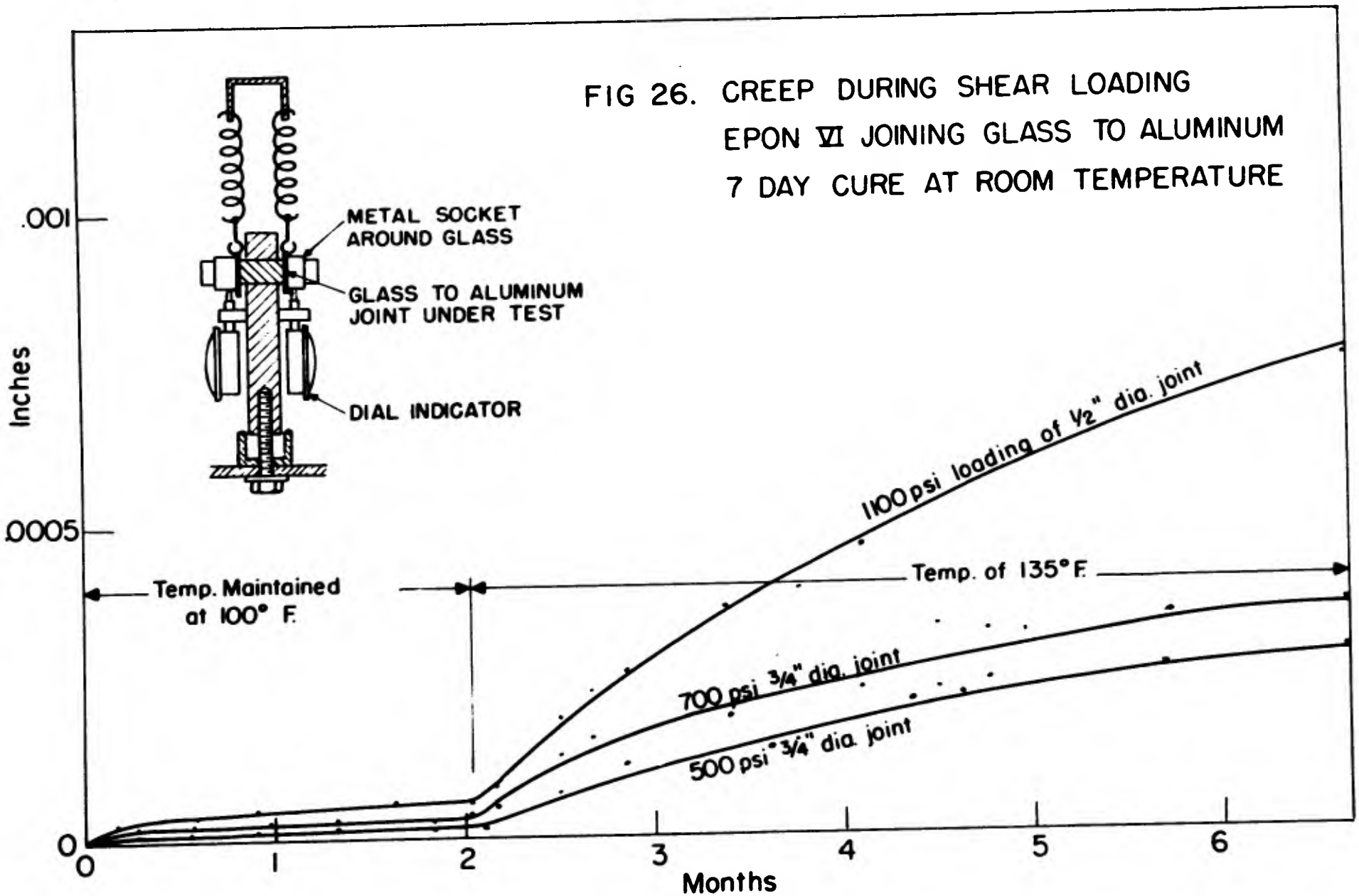

Radiographic Properties of X-rays in the Two- to Six-Million-Volt Range

By C. H. Goldie, K. A. Wright, J. H. Anson, R. W. Cloud, and J. G. Trump

Steady increase in the thicknesses of metal fabrications requiring radiographic inspection dictates the use of higher X-ray energies.

This investigation was prompted by the awareness that the hitherto unexplored X-ray region of from 2 to 6 million volts, still dominated by the Compton absorption process, offered advantages in radiographic speed, sensitivity, and latitude for the examination of heavy metal sections. In 1945 the High Voltage Laboratory under Van de Graaff at the Massachusetts Institute of Technology completed an experimental and analytical study of radiography with 0.5-million to 2-million-volt X-rays (1).[1] The extension of this radiographic study to 6 million volts was supported by the Office of Ordnance Research and was facilitated by the availability at MIT of both a 3-million-volt Van de Graaff X-ray source and the Office of Naval Research Van de Graaff accelerator which covered the 4-million to 6-million-volt X-ray range.

Absorption and Scattering of X-rays

The dominant absorption mechanism in the lower million-volt X-ray range by which photons are diminished in energy and scattered is the Compton effect. In these interactions, dependent primarily on electron density, the photon collides with and imparts energy to an atomic electron, and then proceeds in an altered direction with correspondingly diminished energy. These modified photons are the principal source of scattered radiation.

In this energy range the pair-production mechanism of X-ray absorption in steel is a lesser factor. In this process the photon energy is converted into the rest mass of two electrons which carry away the remainder of the incident photon energy. Pair-production first appears at 1.02 million volts, the rest energy of two electrons, and thereafter increases with photon energy and the atomic number of the absorber. For 6-million-volt photons, for example, pair-production process in iron causes about half as much absorption as Compton process, while in lead, pair-production absorption is about 50 per cent greater than Compton absorption for this energy (2). The positive electron produced in this process disappears at the end of its path by combining with an atomic electron somewhere in the absorber, usually with the emission of two photons of 0.5 million-volts energy. This annihilation radiation is another source of scattered radiation in the high-energy region.

The photoelectric process, which is the principal absorption mechanism for X-rays below 100 kv, particularly with heavy metals, is negligible in the million-volt region.

The direct, or picture-bearing, radiation emerging from an absorber is that portion of the incident radiation still traveling in the original direction. It is the radiation which would emerge if all interactions were complete absorption processes. Unfortunately the scattered radiation produced within the absorber contributes greatly to the emerging radiation, but serves only to fog the film. The total transmitted beam is the sum of this direct and scattered radiation.

A monochromatic direct X-ray beam would be attenuated in an absorber according to the relation

CHARLES H. GOLDIE, Contract Engineering Division, High Voltage Engineering Corp., Cambridge, Mass. Recently engaged in research and development of Van de Graaff accelerators at MIT.

KENNETH A. WRIGHT, High Voltage Research Laboratory, MIT, specializes in application of high energy radiation to biological systems.

JOHN H. ANSON, radiation physicist, Los Angeles Tumor Institute. Former member of the MIT High Voltage Research Laboratory.

ROBERT W. CLOUD, High Voltage Research Laboratory, MIT, engaged in development of Van de Graaff accelerators with emphasis on problems associated with high-voltage acceleration tubes.

JOHN G. TRUMP, Professor of Electrical Engineering and Director of High Voltage Research Laboratory, Massachusetts Institute of Technology. Pioneer in development of the Van de Graaff accelerator as a compact supervoltage radiation source for X-ray therapy.

[1] The boldface numbers in parentheses refer to the list of references appended to this paper.

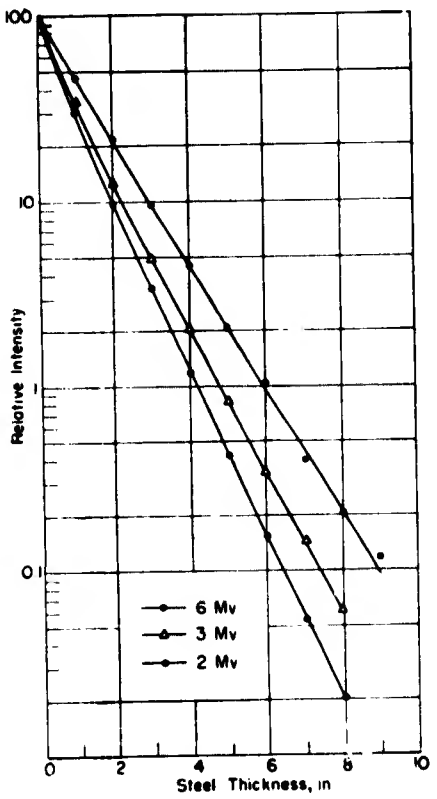

Fig. 1.—Direct-Beam Transmission Curves in Steel for 2-, 3-, and 6-megavolt X-rays.

down to about 0.1 per cent of the incident intensity. It is technically impossible to carry the direct-beam transmission measurements far enough to reach the absorption coefficient of the highest-energy radiation in the beam.

Total-beam transmission curves are quite different in appearance. The total radiation includes both the direct-beam and the scattered radiation which increases rapidly in the first small absorber thicknesses. As seen in Fig. 2, this semilog curve becomes progressively steeper until a few inches of steel have been traversed, after which it becomes virtually straight.

Feshbach (3) has suggested that this straight semilog plot indicates that an equilibrium is reached between the higher-energy components of the transmitted beam and their accompanying scattered secondaries, after which the total beam behaves as if it were a monochromatic beam having an energy equal to the highest energy in the continuous spectrum. It should be noted that at infinite thickness of absorber both the direct- and total-radiation curves should have the same slope.

Within the range of thickness for which accurate detection of the radiation can be accomplished, it has been

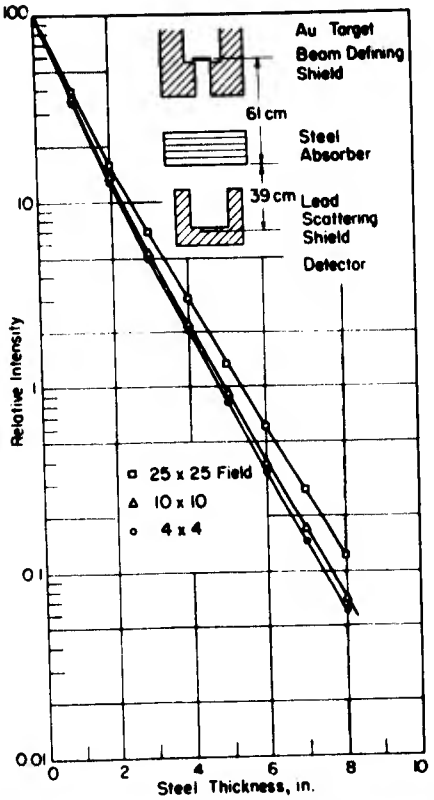

Fig. 3.—3-Megavolt X-ray Transmission Curves in Steel for Different Field Sizes with Direct-Beam Setup.

$$I = I_0 e^{-\mu x} \quad \ldots\ldots\ldots (1)$$

where:

I = the intensity at depth x in the absorber,
I_0 = the incident intensity, and
μ = the linear absorption coefficient.

The logarithm of the monochromatic direct-beam intensity plotted against absorber thickness is a straight line of slope μ.

The continuous radiation spectrum from an X-ray target contains photons of all energies up to the maximum tube voltage. Since the linear absorption coefficient, μ, diminishes steadily with increasing photon energy (until about 7 million volts for iron), the selective absorption of the less energetic photons shifts the spectrum of the direct radiation toward the short wavelength limits. This shift toward the high-energy end of the spectrum soon becomes extremely slow; the direct-beam transmission curve plotted as in Fig. 1 becomes almost a straight line, and the beam behaves as essentially monochromatic radiation. Thus, any direct X-ray beam, after sufficient initial absorption, can be described by an effective absorption coefficient, μ_D. The value of μ_D is usually obtained from direct-beam curves which extend

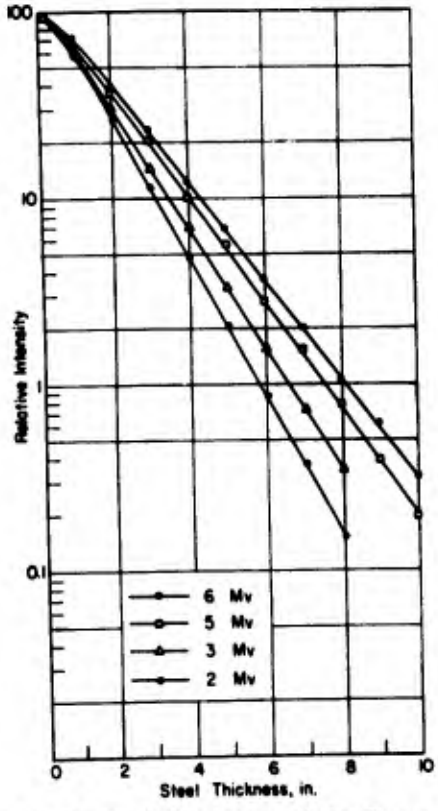

Fig. 2.—Total-Beam Transmission Curves in Steel for 2-, 3-, 5-, and 6-megavolt X-rays with a 25 by 25-cm Field.

experimentally found for 1- and 2-million-volt X-rays that the ratio of the scattered radiation to the direct is proportional to the thickness of the absorber (4).

Experimental Apparatus and Procedure

The X-rays from both Van de Graaff accelerators had an equivalent filtration of about 11 mm of lead, most of which was in the ¼-in.-thick gold targets. With the ONR[1] generator, working space was gained by magnetically deflecting the electron beam through 90 deg before allowing it to strike the target. The 3-million-volt X-ray generator was calibrated for negative operation, and the two lower voltages, which were obtained with this machine, are known to an accuracy of better than ±3 per cent. Although the ONR machine was very accurately calibrated for positive ion operation, estimated accuracy for its operation as an X-ray source for the 5- and 6-million-volt data is ±5 per cent.

The X-ray energy incident on the absorber was monitored with a thin-wall flat ionisation chamber placed in the field close to the X-ray target

[1] Financed by the Office of Naval Research, operated by the MIT Laboratory of Nuclear Science and Engineering.

and connected to a remote modified Shepard-Roberts d-c amplifier. A special flat ionization chamber with adjacent preamplifier and remote amplifier and indicating circuit was used to measure the transmitted intensity. This detector was shaped to approximate the conditions of actual radiography, the mean depth of its thin, flat air cavity being about the same distance beneath the bottom of the steel plates as a film in a pressure cassette.

For the direct-beam measurements, the detector was placed remote from the steel absorber and surrounded with a 3-in.-thick lead shield to reduce approaching scattered radiation. The 2- and 3-million-volt transmission curves were obtained with fields defined to 4 by 4, 10 by 10, and 25 by 25 cm at the detector with setup dimensions as indicated in the inset of Fig. 3. The 3-million-volt curves are shown in Fig. 3. The small difference between the transmission of the two smaller fields suggests that the 4 by 4-cm data can be accepted as the direct-beam curve with only small error. Because of the poorer electron-beam focus in the ONR accelerator, the field size used for the direct-beam measurements at 5- and 6-million volts was increased to 6 by 6 cm, the target-to-detector distance increased from 100 to 135 cm, and the distance from absorber to detector from 39 to 62 cm. Under these conditions the detector chamber had a somewhat smaller solid angle for scatter from the steel plates.

The total-beam data were taken for three fields for the two lower voltages and for two fields for the higher voltages. In these measurements the target-to-detector distance remained the same as in the direct-beam situation, but the steel was stacked directly against the lead block containing the detector. This lead block, in which the chamber was embedded, provided protection from general room scatter. In practice this is also done to the film cassette in a radiographic setup.

Results of Direct- and Total-Beam Measurements

Figure 1 shows the direct radiation as a function of steel thickness for 2-million, 3-million, and 6-million-volt X-rays. The focus of the electron beam in the ONR machine had been adjusted for 6-million-volt operation and was left unadjusted at 5-million volts with resultant defocusing and error in the 5-million-volt direct-beam data. Unavailability of the ONR machine prevents the repetition of this run. The direct-beam curves are sufficiently straight to permit the calculation of an absorption coefficient and an "equivalent energy." Table I lists the direct-beam linear absorption coefficient, μ_D, and the energy in million-electron-volt units of the monochromatic radiation which would have the same absorption coefficient.

TABLE I.—EFFECTIVE ABSORPTION COEFFICIENT AND "EQUIVALENT ENERGY" OF DIRECT BEAM.

Tube Voltage, megavolts	Direct Beam Absorption Coefficient, μ_D, in.$^{-1}$	Equivalent Monochromatic Energy, mev
2.....	1.04	1.30
3.....	0.90	1.75
6.....	0.77	2.50

Figure 4 shows the total transmitted radiation as a function of thickness for 4 by 4, 10 by 10, and 25 by 25-cm fields of 3-million-volt X-rays, and Fig. 2 shows the total transmitted radiation for the 25 by 25-cm field with 2-, 3-, 5-, and 6-million-volt X-rays. The plots are essentially straight lines on the semilog paper. These two figures demonstrate the considerable dependence of total transmitted radiation on both field size and voltage. The total-beam absorption coefficients calculated from the slopes of the 25 by 25-cm data in Fig. 2 are compared in Table II with the theoretical absorption coefficients for a monochromatic beam with energy equal to the maximum energy of the continuous spectrum (*2*). The fairly close check is similar to that found by the Office of Scientific Research and Development group for 1- and 2-million-volt X-rays with a 25-cm diam round field, and is in agreement with Feshbach's theory. It is probable that a larger field must be used to approximate the condition of irradiating an absorber with an infinite field in order to bring about Feshbach's "equilibrium distribution." Even so, the total-radiation semilog plots are close to straight lines, although the measured absorption coefficient remains slightly higher than the limiting value for that voltage.

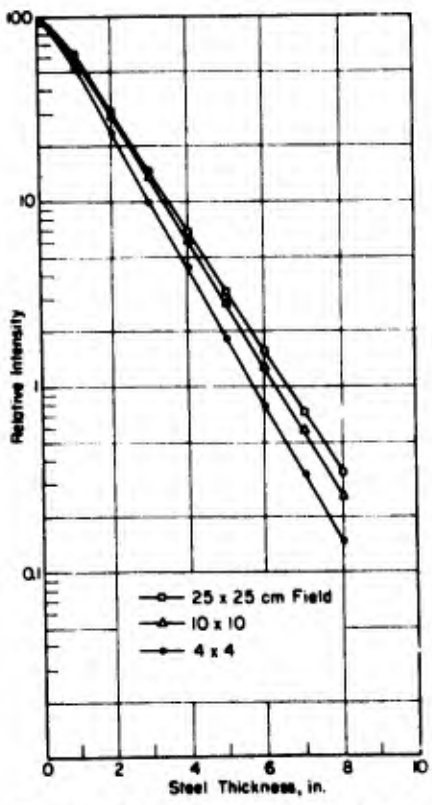

Fig. 4.—3-Megavolt Total X-ray Transmission Curves in Steel for Different Field Sizes.

X-ray Intensity and Exposure Time

Since most radiography is done with fields at least as large as 25 by 25 cm, this field size and a commonly used high-quality film, Eastman Type A Industrial Radiographic Film, were chosen for the calculation of an exposure chart. Type A film requires a radiation dose of 4 roentgens to produce a film density of 3. This dose is practically independent of radiation energy above about 300 kev[3] (*5*). A density of 3 was selected because a chart constructed for this density combined with the latitude curves makes it simple to determine the maximum thickness that can be radiographed at a particular tube voltage with a sensitivity of 1 per cent. This computation is described in a later paragraph.

[3] Unpublished data of R. Granke, High Voltage Research Laboratory, Electrical Engineering Dept., Massachusetts Institute of Technology.

TABLE II.—TOTAL BEAM ABSORPTION COEFFICIENT AND SCATTERING FACTOR.

Tube Voltage, megavolts	Total Beam Absorption Coefficient for 25 by 25-cm Field, μ, in.$^{-1}$	Calculated Absorption Coefficient of Monochromatic Radiation of Maximum Energy, in.$^{-1}$	Scattering Factor, k, in.$^{-1}$	k/μ
2.....	0.86	0.84	0.80	0.93
3.....	0.75	0.72	0.56	0.75
5.....	0.66	0.62	...	...
6.....	0.61	0.60	0.41	0.67

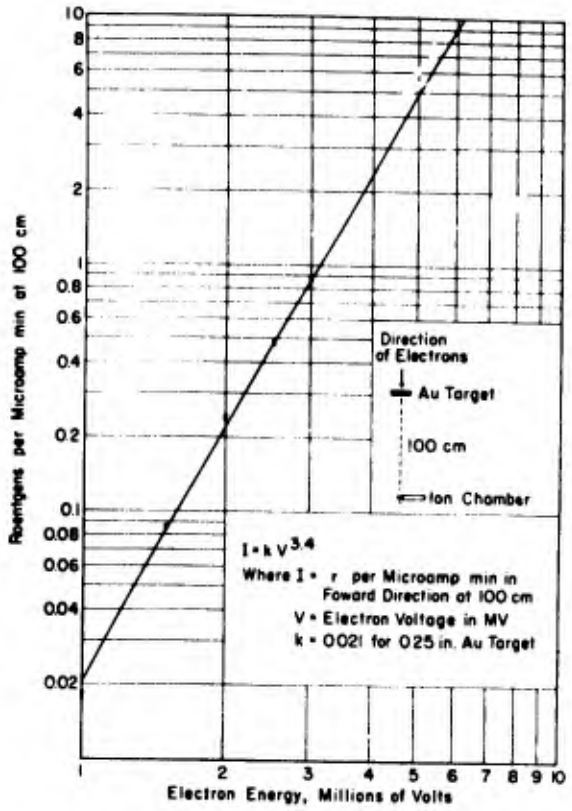

Fig. 5.—Radiation Output *versus* Electron Energy in megavolts.

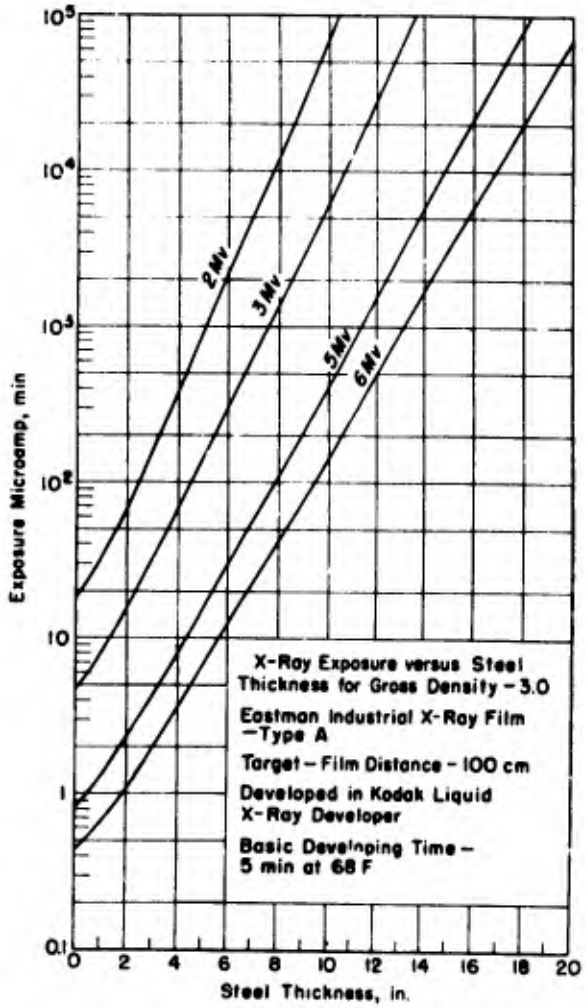

Fig. 6.—Exposure Chart for 2-, 3-, 5-, and 6-megavolt X-rays with Eastman Type A Industrial X-ray Film.

The zero-thickness exposure points on the chart require a knowledge of the output intensity at each voltage. Figure 5 is a plot of output X-ray intensity in roentgens per μa-min at 1 meter as measured on the 3-million-volt X-ray generator. This shows that the output intensity is proportional to the 3.4 power of the voltage in the range from 1 million to 3 million volts. The data were taken with a Victoreen condenser r-meter chamber covered with a Lucite cap thick enough to produce electron equilibrium with the X-radiation. Although absolute measurements of the X-ray output could not be made on the ONR machine because of the lack of knowledge of the actual target current, relative measurements indicated that the 3.4 power of the voltage rule held to the highest voltage. Therefore, the zero thickness points for the two higher voltages were taken from an extrapolation of the curve. From zero thickness up, the exposure curves of Fig. 6 are the inverse of the 25 by 25-cm total-beam transmission plots. If one prefers to use a lower density or a different film, correct exposures can be computed by multiplying the value given on the chart by a constant factor obtained from film-response curves. It should be noted that the exposure curves will apply accurately only with lead intensifying screens of sufficient thickness to produce electron equilibrium with the X-radiation.

Scattering Factor

Calculations of radiographic sensitivity for the various voltages first require determination of the scattering factors. The scattered radiation was found by subtracting the direct from the total radiation for each thickness. The ratio of the scattered to the direct radiation was then plotted against steel thickness for each voltage; the resultant curves in Fig. 7 are approximately linear. The scattering factors, k, for 2-million, 3-million, and 6-million volts, are the slopes of these curves and are listed in Table II. Although there is a 25 per cent difference between the new and the OSRD values of the scattering factor for 2-million-volt X-rays, the expected diminishing improvement with increasing voltage is qualitatively shown. Table II also lists the values of k/μ, a factor often used as an index of radiographic merit as discussed below.

Radiographic Sensitivity

Since sensitivity is the minimum observable thickness variation expressed as a percentage of the total thickness of the absorber, it is desirable to have a low sensitivity. Scattered radiation plays its major rôle in adversely affecting sensitivity. Without scatter, the radiation intensity on a film under an examined object would depend at each point only on the thickness, x, of metal directly above that point. In this idealized situation the sensitivity would be

$$S = \frac{2.3\alpha}{\gamma\mu x} \quad \ldots\ldots\ldots\ldots (2)$$

where:

α = the minimum observable film density difference, usually taken to be 0.008, and

γ = the film gamma or slope of the curve of film density *versus* $\log_{10}$ relative exposure.

Equation 2 indicates that low-voltage X-rays with their correspondingly

higher absorption coefficients would give the best sensitivities. However, scatter cannot be eliminated in practice. Placing the film remote from the absorber or using a moving grid between the absorber and film to block out oblique radiation greatly reduces the scatter to the film but causes a loss of definition and increased exposure and setup time.

The expression for sensitivity, including the effect of scattered radiation (6), is

$$S = \frac{2.3\alpha}{\gamma\mu x}(1 + kx) = \frac{2.3\,x}{\gamma\mu x}\left(\frac{T}{D}\right) \quad (3)$$

where:

D = the direct radiation, and
T = the total radiation at depth x.

Thus, sensitivity with scatter is equal to sensitivity without scatter multiplied by the ratio of the total radiation to the direct. If the direct beam could be used free of scatter, the detectable thickness difference would be constant and would depend only on the film contrast and the absorption coefficient. This condition of "absolute sensitivity" is approximately realized for th[illegible] extremely high-volta[illegible] X-[illegible].

With large thicknesses, [illegible] ensitivity with scatter approaches the constant value

$$S_\infty = \frac{2.3\alpha k}{\gamma\mu} \quad (4)$$

For this reason the value k/μ has become recognized as an index of the radiographic quality of a beam of X-rays. Qualitatively, k/μ increases with voltage to a maximum at about 0.5 million volt, after which it decreases rapidly at first and then more slowly. Thus, sensitivity actually improves with increasing voltage above 0.5 million volt, and is still improving slowly in the 2- to 6-million-volt region.

Use of the experimental values for the scattering factors in Eq 3 for sensitivity results in the curves shown in Fig. 8. These curves were calculated on the basis of a film gamma of 6 (Eastman Type A film) and α of 0.008. It is clearly shown that the sensitivity for sections thicker than 4 in. is better for 6-million volts than for 3. However, this gain is small compared with that obtained in going from 0.5-million volt to 2-million volts, or even from 2- to 3-million volts.

The sensitivities discussed above are for the ideal case of flat plates. Actual objects to be radiographed vary in shape, and the calculation of the sensitivity can be extremely involved. The alternative form of the sensitivity equation can be used for any point on the radiograph where the ratio of the total to the direct radiation can be determined. A discussion of methods for making approximate calculations of this type is contained in a thesis by Hornbeck (7) as well as in the OSRD report (8). Where very small fields can be used to examine details of objects, it is possible to obtain lower sensitivities because of the resultant decrease in scattered radiation.

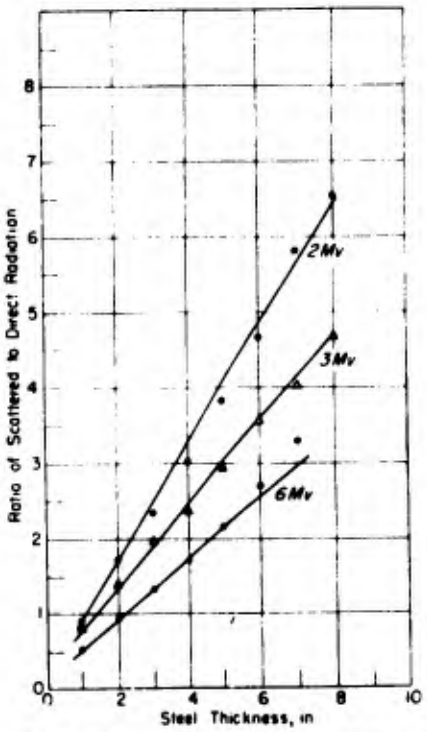

Fig. 7.—Ratio of Scattered-to-Direct Radiation *versus* Steel Thickness for 2-, 3-, and 6-megavolt X-rays.

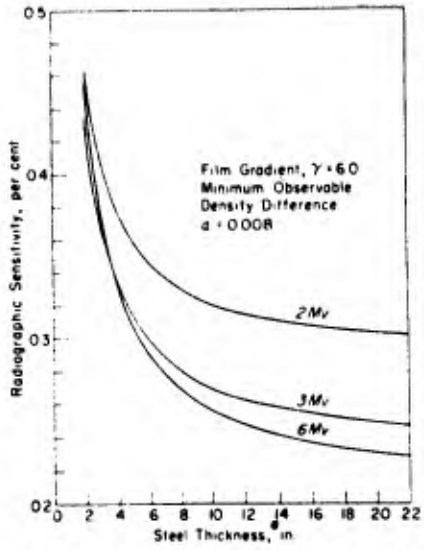

Fig. 8.—Sensitivity *versus* Steel Thickness for 2-, 3-, and 6-megavolt X-rays. 25 by 25-cm Field.

Latitude

Radiographic latitude refers to the thickness range that can be examined with good sensitivity in a single exposure. For steel thicknesses in the straight-line region of the total-beam transmission curves, the following equations hold:

$$\epsilon_{min} = \epsilon_0 e^{-\mu L}$$

$$L = \frac{2.3}{\mu}\left[\log_{10}\epsilon_0 - \log_{10}\epsilon_{min}\right] \quad (5)$$

where:

ϵ_0 = film exposure to give a density of 3 with a given steel thickness,
ϵ_{min} = film exposure for the minimum film density required to give a sensitivity of 1 per cent, and
L = latitude, defined here as that additional thickness of steel examined with a film density sufficient for a sensitivity of 1 per cent when the given thickness is examined with a density of 3.

The difference expressed in the brackets of Eq 5 can be found for each steel thickness in the following way: The minimum values of film gamma, γ, are calculated by substituting $S = 0.01$ in Eq 3 and solving for different thicknesses. Then the required densities are found from a curve of γ *versus* density for the film used (9). Finally, the difference in log exposure for density 3 and for each minimum density is given by the characteristic curve of the film. This definition of latitude is similar to that adopted by the OSRD group. The selection of a maximum sensitivity of 1 per cent was arbitrary, and the maximum density of 3 was chosen since this is the upper limit of ordinary fluorescent viewers. Although the latitude is certainly increased by the use of greater densities and high-intensity viewers, the present definition is sufficient for a comparison of the latitudes obtained with different tube voltages. The curves of latitude *versus* steel thickness shown in Fig. 9 were obtained by such calculations for type A film.

Maximum Steel Thickness

The maximum steel thickness that can be effectively radiographed in a reasonable time with each tube voltage can be determined by using Fig. 6 in conjunction with Fig. 9. If one assumes a reasonable maximum exposure, Fig. 6 will give for each voltage the steel thickness through which a film density of 3 can be obtained. Adding the latitudes from Fig. 9 to these numbers gives the maximum thicknesses that can be radiographed with a sensitivity of 1 per cent.

If we assume 1.5×10^4 μa-min, or

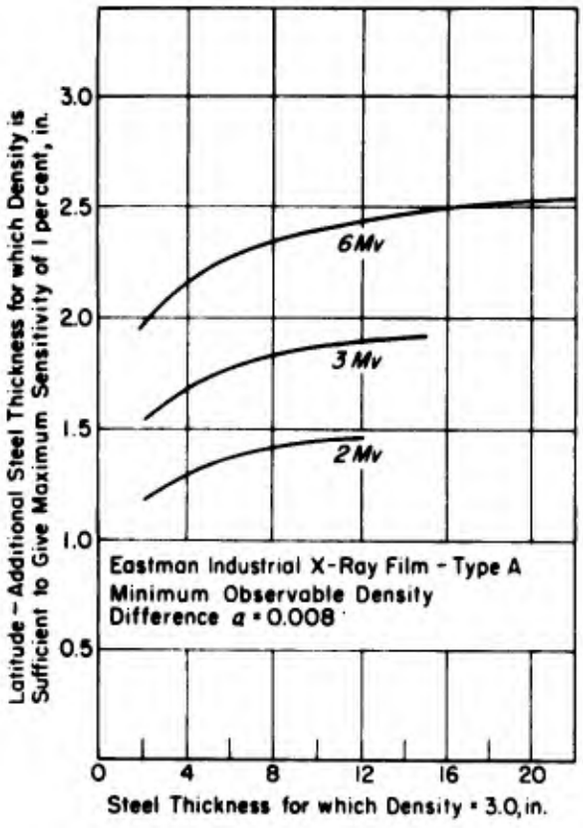

Fig. 9.—Latitude *versus* Steel Thickness for 2-, 3-, and 6-megavolt X-rays. 25 by 25-cm Field.

1 hr at 250 μa, as a practical maximum exposure, the maximum steel thickness is found to be 9.5 in. for 2-million-volt X-rays, 13 in. for 3-million volts, and 20 in. for 6-million volts. These figures are increased somewhat by the use of faster film and shorter target-to-film distance. An example of the gain in speed with voltage is to note that the 20 min required for 7 in. of steel at 2-miilion volts would be reduced to 2.5 min at 3-million volts, 14 sec at 5-million volts, and 5.5 sec at 6-million volts.

Definition

Definition refers to the sharpness of reproduction on a film of a particular discontinuity in the radiographed object. Simple geometric considerations result in

$$c = \frac{st}{d} \quad \ldots\ldots\ldots\ldots (6)$$

where:

c = the diameter of circle of confusion,
s = the diameter of focal spot,
d = the target-to-defect distance, and
t = the defect-to-film distance.

A dimensionless point in the object will appear as a circle of diameter, c, in the radiograph. For a sharp picture it is important to have a small focal spot and as large a ratio of d/t as is reasonable from the point of view of exposure time. Since the electron beam from a Van de Graaff accelerator is homogeneous in energy, a simple annular magnet around the tube extension can be used to focus the spot to minimum diameters of the order of 0.01 in. (6, p. 61). Other factors beside geometry that ultimately limit the resolution of the radiograph are the film grain size and the range of the secondary electrons in the emulsion. The average grain size is about 0.004 in. for Eastman Type A, a relatively fine-grain X-ray film. Only pair-production and Compton electrons, which are scattered at wide angles to the X-ray beam, are effective in spreading the image in the emulsion. Although the energy of these electrons increases with photon energy, the probability of their having wide angles decreases. The limit in resolution caused by the range of these electrons at 2-million volts is also about 0.004 in. (6, p. 61). Although this limit has increased at 6-million volts, substantially higher voltages are required to make this phenomenon a practical limitation.

Summary

1. The principal radiographic properties of X-rays produced by electrons in the energy range from 2-million to 6-million volts have been investigated for the first time.

2. The expected large increase in radiographic speed and the progressively smaller improvement in sensitivity as the voltage is increased from 2-million to 6-million volts are experimentally confirmed.

3. It is evident that a nearly optimum balance of radiographic properties for the investigation of thick metal sections is found in the energy range from 2 million to 6 million volts. Further substantial increases in X-ray voltage would result in increased range of secondary electrons, a diminution of available field size, and a slow increase of absorption coefficient due to pair-production.

Acknowledgment:

This work was performed as part of the work under the Office of Ordnance Research Contract DA-19-020-ORD-2023, the support of which is gratefully acknowledged. The assistance of Bjorne Aarset, Sanborn F. Philp, Herbert Weiss, and G. Y. Chu on measurements with the ONR accelerator is also much appreciated.

References

(1) "Final Report on the MIT Project in High-Voltage Radiography," Office of Scientific Research and Development, National Defense Research Committee, *OSRD Report No. 4488*, June 1, 1945.
(2) C. M. Davisson and R. D. Evans, "Gamma-Ray Absorption Coefficients," *Reviews of Modern Physics*, Vol. 24, April, 1952, pp. 79–107.
(3) *OSRD Report No. 4488*, Vol. 4, Ch. 3c (1945).
(4) *OSRD Report No. 4488*, Vol. 4, Ch. 3b (1945).
(5) E. Storm, "Response of Film to X-Radiation of Energy Up to 10 MeV," Los Alamos Scientific Laboratory of the University of California, *Report No. LA 1220*, May 16, 1950.
(6) W. W. Buechner, R J. Van de Graaff, H. Feshbach, E. A. Burrill, A. Sperduto, and L. R. McIntosh, "An Investigation of Radiography in the Range from 0.5 to 2.5 Million Volts," *ASTM* Bulletin, No. 155, December, 1948, p. 54.
(7) J. A. Hornbeck, Ph.D. Thesis, Massachusetts Inst. of Technology (1944).
(8) *OSRD Report No. 4488*, Vol. 4, Ch. 4e (1945).
(9) Eastman Kodak Co., "Radiography in Modern Industry," Rochester, N. Y., p. 87 (1947).